

# FUNOff: Offloading Applications at Function Granularity for Mobile Edge Computing

Xing Chen<sup>1</sup>, Member, IEEE, Ming Li, Hao Zhong<sup>1</sup>, Member, IEEE, Xiaona Chen, Yun Ma<sup>1</sup>, Member, IEEE, and Ching-Hsien Hsu<sup>2</sup>, Senior Member, IEEE

**Abstract**—Mobile edge computing (MEC) offers a promising technology that deploys computing resources closer to mobile devices for improving performance. Most of the existing studies support on-demand remote execution of the computing tasks in applications through program transformation, but they commonly assume that mobile devices merely resort to a single server for computation offloading, which cannot make full use of the scattered and changeable computing resources. Thus, for object-oriented applications, we propose a novel approach, called FUNOff, to support the dynamic offloading of applications in MEC at the function granularity. First, we extract a call tree via code analysis and locate the function invocations that are suitable for offloading. Next, we refactor the code of related object functions according to a specific program structure. Finally, we make offloading decisions referring to the context at runtime and send function invocations to multiple remote servers for execution. We evaluate the proposed FUNOff on two real-world applications. The results show that, compared with other approaches, FUNOff better supports the computation offloading of object-oriented applications in MEC, which reduces the response time by 10.7%–58.2%.

**Index Terms**—Mobile edge computing, computation offloading, code analysis, object-oriented application, software adaptation.

## I. INTRODUCTION

With the rise of intelligent technologies, massive computation-intensive applications (e.g., autonomous driving [1], image recognition [2], and augmented reality [3]) have been developed to improve the quality of people's life. However, most existing smart devices (e.g., wearable devices [4], vehicles [5], and UAVs [6]) are unable to handle computation-intensive tasks in a short time due to the constraints

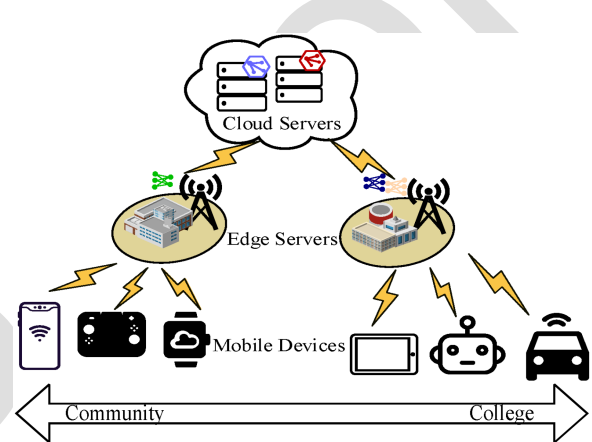


Fig. 1. Mobile edge computing (MEC) architecture.

on their processing power, memory capacity, and battery capacity [7].

Computation offloading is an effective way to resolve resource constraints on mobile devices [8]. In the last decade, one feasible way is to offload computation-intensive tasks from mobile devices to a cloud server, aiming to improve the performance of mobile applications [9], [10], [11]. This paradigm is known as mobile cloud computing (MCC). Although MCC elevates user experience, higher network delay can happen, if the cloud server is remote [12]. Meanwhile, the massive data transmission between the cloud server and mobile devices increases the traffic load of core networks [13]. When there are many mobile devices, the performance of MCC may be seriously affected, especially for latency-sensitive applications. To further improve MCC, a new paradigm, called mobile edge computing (MEC) has emerged. Fig. 1 depicts a typical MEC architecture: there is a three-tier computing architecture consisting of mobile devices, edge nodes, and the cloud [14], [15]. By pushing the computing resources from the centralized cloud to the decentralized edges near the data source (e.g., mobile devices), MEC reduces the influx of data on the backbone [16], [17]. Therefore, MEC has been regarded as a more effective way to reduce the service delay than MCC does.

Due to the geographical distribution of MEC servers and the mobility of mobile devices, the runtime context in MEC is highly complex and dynamic [18], [19]. Although the prior studies [20], [21], [22] can be extended to the scenario of MEC, they lack enough effectiveness, since they only divide an application into

Manuscript received 11 May 2022; revised 11 January 2023; accepted 19 January 2023. This work was supported in part by the National Natural Science Foundation of China under Grant 62072108 and in part by the Natural Science Foundation of Fujian Province for Distinguished Young Scholars under Grant 2020J06014. Recommended for acceptance by Dr. J. Wu. (Corresponding author: Hao Zhong.)

Xing Chen, Ming Li, and Xiaona Chen are with the College of Computer and Data Science, Fujian Provincial Key Laboratory of Network Computing and Intelligent Information Processing, Fuzhou University, Fuzhou 350118, China (e-mail: chenxing@fzu.edu.cn; 210310011@fzu.edu.cn; cxn\_95@163.com).

Hao Zhong is with the Department of Computer Science and Engineering, Shanghai Jiao Tong University, Shanghai 200240, China (e-mail: zhonghao@sjtu.edu.cn).

Yun Ma is with the School of Electronics Engineering and Computer Science, Peking University, Beijing 100871, China (e-mail: mayun@pku.edu.cn).

Ching-Hsien Hsu is with the Department of Computer Science and Information Engineering, Asia University, Taichung 413, Taiwan (e-mail: robertchh@gmail.com).

Digital Object Identifier 10.1109/TMC.2023.3240741

63 two parts and deploy them on a mobile device and a remote  
 64 server. In our prior work, we propose an adaptive offloading  
 65 architecture, called Androidoff [23], [24]. Androidoff is able  
 66 to offload applications among the local device, mobile edges,  
 67 and the cloud dynamically, but it still reveals the following  
 68 limitations:

69 (1) There is still improvement space for the performance of  
 70 Androidoff. The Androidoff offloads applications at the granu-  
 71 larity of objects, but it would be more flexible by adopting finer  
 72 granularity. For example, an object owns two methods, which  
 73 intend to be offloaded to the edge and the cloud, respectively.  
 74 However, since these two methods are from the same object,  
 75 they can only be offloaded to the same location (i.e., the edge or  
 76 the cloud).

77 (2) When users move to a new location, Androidoff ensures  
 78 the normal operation of applications by accessing the copied ob-  
 79 jects of the cloud server. If the new environment is not connected  
 80 to the cloud server, some information may be lost, which causes  
 81 crashes. Meanwhile, the time of restarting applications is often  
 82 unacceptable.

83 Although it is beneficial to offload applications at a finer  
 84 granularity, it is challenging to decompose applications. Most  
 85 applications are monolithic and have a high degree of internal  
 86 coupling [25]. Moreover, another challenge is to avoid loss of  
 87 information when users move to new scenarios. Mobile devices  
 88 need to maintain all the state information of the objects to ensure  
 89 that the application can keep executing normally.

90 Recently, the Function as a Service (FaaS) programming  
 91 model has been widely adopted with the emergence of serverless  
 92 cloud computing [26], [27]. In FaaS, an application is split into  
 93 short-lived stateless functions that can be executed by different  
 94 computing nodes [28], which is a fine-grained computation  
 95 offloading. The basic idea of FaaS can resolve the problem  
 96 of information loss caused by a finer granularity. However, to  
 97 realize this idea, there are two key challenges: (1) The execution  
 98 of a function in an object-oriented (OO) application depends on  
 99 the states of multiple objects. (2) To adapt to the highly complex  
 100 and dynamic runtime context of MEC, an algorithm shall make  
 101 quick offloading decisions.

102 To address the problems of the state-of-the-art, we propose a  
 103 novel offloading mechanism, called FUNOff. The major contribu-  
 104 tions of this paper are as follows:

- 105 • A novel offloading mechanism, called FUNOff, that sup-  
 106 ports the offloading of applications at the granularity of  
 107 functions. The FUNOff builds a call tree, and discovers  
 108 function invocations that are suitable for offloading. To  
 109 resolve the state dependencies of methods, the FUNOff  
 110 transforms functions into stateless ones based on the code  
 111 analysis results.
- 112 • An online decision traversal strategy that uses the prop-  
 113 erties of the call tree and the tendency of computation  
 114 offloading to synthesize offloading schemes.
- 115 • Extensive evaluation results on two real-world applica-  
 116 tions. We evaluate FUNOff on License Plate Recogni-  
 117 tion Application (LPRA) and Target Detection Application  
 118 (TDA). Compared with the existing approaches [9], [23],  
 119 [24], the results show that FUNOff reduces the response

time of LPRA and TDA by 10.7%-45.7% and 14.5%-  
 58.2%, respectively.

## II. RELATED WORK

A. *Offloading Mechanism*

Computation offloading is a way to resolve resource constraints on mobile devices. The state-of-the-art offloading mechanism can offload applications by the granularity of program fragments [11], methods [9], [20], [21], classes [29], layers [22], and objects [23], [24].

Cuckoo [11] is a computation offloading framework with the granularity of program fragments. It asks developers to comply with a given programming paradigm to refactor the application so that certain parts of it can be offloaded to the cloud server. DPartner [29] can offload classes, and it uses a proxy mechanism to access class instances. Further, it calculates the coupling of classes and deploys them in two parts on a mobile device or a remote cloud server. Although the above approaches can effectively support computation offloading of applications in MCC, they are not designed for MEC. MAUI [9] is a computation offloading framework for C# applications, which offloads applications at the granularity of methods. The programmers only need to mark remoteable methods, and the application can be restructured automatically. Then the framework will decide which methods should be offloaded to the remote server at runtime. ULOOF [20] also works on the granularity of methods, but it targets the offloading problem for Java applications. Dandelion [21] is a unified code offloading system for wearable computing that supports multi-process offloading. It can generically offload tasks to a cloud, a cloudlet, or nearby smart devices. DeepWear [22] strategically offloads DL tasks from a wearable device to its paired handheld device. It splits a DL model into two sub-models that are first executed on the wearable and then on the handheld. However, the above studies only divide the application into two parts and deploy them on a mobile device and a remote server, respectively. This paradigm cannot support the dynamic offloading among the device, mobile edges, and the cloud [30], [31], [32], which limits performance improvement. To address this issue, AndroidOff [23], [24] proposed an adaptive offloading framework that supports computation offloading at the object granularity in MEC. It enables offloading applications among the local device, mobile edges, and the cloud dynamically. However, the stateful nature of the methods makes AndroidOff inapplicable in some scenarios.

## B. *Offloading Strategy*

Computation offloading needs to determine which parts of an application shall be offloaded and to which compute nodes, i.e., the decision of an offloading scheme. A qualified offloading scheme needs to balance the impact of various factors, such as computing performance and network environment, around the offloading goal. In recent years, researchers have started to explore the intelligent scheduling of computation offloading in MCC or MEC.

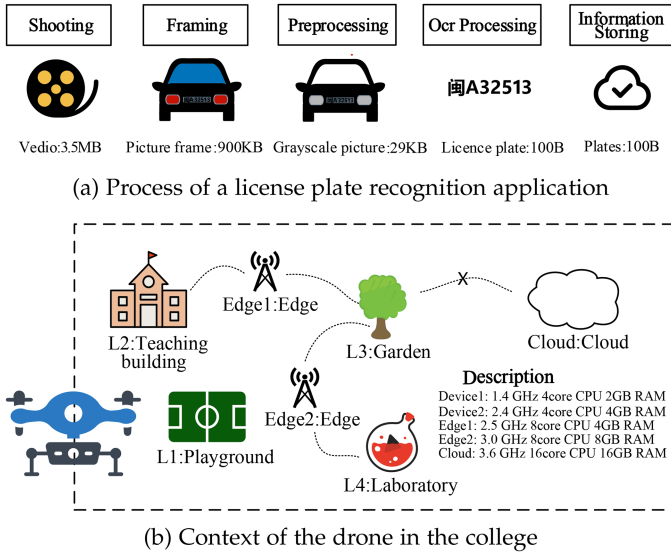


Fig. 2. The sample scenario (a) Process of a license plate recognition application. (b) Context of the drone in the college.

Altamimi et al. [33] evaluated the communication energy consumption of offloading computing tasks to cloud servers and established a high-precision energy consumption estimation model without the requirement of complete input parameters. It can decide whether computing tasks shall be offloaded based on this model rapidly. Elgazzar et al. [34] proposed a framework for collaborative offloading services to provide computation offloading services for mobile devices based on the system network, resource status, and energy consumption constraints. Zhou et al. [35] proposed a context-aware offloading decision algorithm to provide offloading decisions at runtime, called mCloud, which selects a wireless medium and appropriate cloud resources for offloading. The works [33], [34], [35] aim at intelligent scheduling in MCC, and some works [30], [36] are proposed for MEC. Cheng et al. [30] proposed a three-layer computation offloading framework composed of wearable devices, mobile devices, and edge nodes. They introduced genetic algorithms to increase the task throughput of wearable devices in MEC. Wu et al. [36] proposed a task partition algorithm suitable for the computation offloading of graph applications. They adopted an improved bipartite graph algorithm to divide the computing tasks into local and remote ones. However, the above approaches make offloading decisions based on the high-level abstract model of a program, rather than a real application.

### III. MOTIVATION

MAUI [9] is a well-known computation offloading framework, which supports the dynamic offloading of object-oriented programs at method granularity in MCC. It allows annotating which methods can be offloaded beforehand and deciding the offloading scheme at runtime. AndroidOff [23], [24] is an adaptive offloading framework for MEC. It is designed to handle object-oriented programs and offload them at the object granularity. In this section, we use a scene as shown in Fig. 2 to illustrate how MAUI [9], AndroidOff, and FUNOff work. In this scene,

the drone cruises around the college, and when it detects illegal parking, the LPRA in the drone will be operated to identify the car's plate number from the video stream. Fig. 2(a) shows the process of LPRA, including shooting, framing, preprocessing, ocr processing, and information storing. Each process contains several functions, as shown in Fig. 7(a). These tasks require different computation power. For example, ocr processing is a computation-intensive task, and it is more effective to offload it to a remote server; meanwhile, framing exhibits low computation complexity. The data traffic between tasks is another influencing factor. For example, the data traffic between shooting and framing is large, while between preprocessing and ocr processing is marginal. It is preferred to execute two adjacent tasks with high data traffic on the same device. Fig. 2(b) shows the context of the drone when it cruises around the college. There are three available remote servers (Cloud, Edge1, and Edge2) in different locations. Edge1 is located in the teaching building and the garden; Edge2 can be accessed from the garden and the laboratory; Cloud can be accessed from other locations besides the garden. Notes that the network environment and the LPRA are the same as the setting in Section V. To improve the performance, when the drone stays in different locations, it needs to determine where each computation task is executed and then offload each task to its corresponding server in a real-time manner. When the drone moves to a different location, its application must be smoothly switched between servers.

We discuss two offloading cases:

Case 1: When the drone stays in a location, it must be able to utilize the scattered computing resources around the location. For example, the drone can use a cloud server and an edge server to improve the performance of LPRA in the Laboratory. In this location, FUNOff offloads computation-intensive functions such as RecInEachChar.getHZ() and Orientation.math() to the cloud or edge by comparing the reduced execution time with the increased network latency. If functions implement simple tasks, they are executed locally. As for MAUI only uses a single remote server for computation offloading due to its poor scalability. It cannot offload different methods to multiple different remote servers to further enhance performance, so RecInEachChar.getHZ() and Orientation.math() are both offloaded to the edge server. As a result, MAUI can only reduce the response time by 34%, while FUNOff can reduce it by 46%. According to our offloading scheme, getHZ() and GetRegion() are executed on the cloud and drone, respectively. AndroidOff is offloaded at object granularity, getHZ() and GetRegion() can only be offloaded to the cloud since they are both methods of object RecInEachChar.

Case 2: When the drone moves between different locations, it shall switch smoothly. For example, suppose that the drone moves from the teaching building to the garden. In the beginning, the drone executes the LPRA in the teaching building. It offloads the function RecInEachChar.getHZ() to Cloud according to our offloading scheme. During the application execution, the drone moves to the garden, causing the application to disconnect from Cloud. Since both FUNOff and MAUI save the information of the object RecInEachChar in the drone, they can ensure the normal execution of RecInEachChar.getHZ() in the new context.

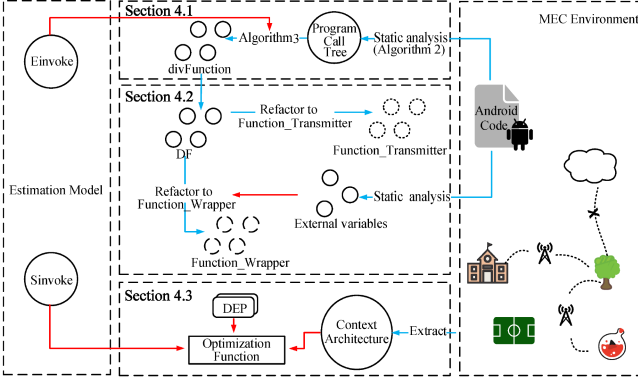


Fig. 3. The overview of FUNOff.

As Androidoff takes the object as the minimum offloading unit, the state information of the object is saved on the corresponding execution location. The application will crash when the drone moves from the teaching building to the garden. The information of the object RecInEachChar is not saved on the drone, and there is no connection to the Cloud to get the information. As a result, the crash caused 20s delay in restarting the application. In order to make offloading smoother, the generation time of offloading schemes needs to be reduced. FUNOff can reduce it by determining the appropriate cut-point functions in advance.

Compared with the above approaches, FUNOff has the following main improvements: (1) it can support adaptive offloading at function granularity in MEC; (2) The object methods are translated into stateless functions to avoid the loss of state information caused by movement. (3) To support offloading at runtime, the set of cut-point functions suitable for offloading is automatically determined in advance to reduce the generation time of the offloading scheme.

#### IV. APPROACH

Fig. 3 shows the overview of FUNOff. The FUNOff reuses the estimation model of AndroidOff proposed in our previous work [23]. This model predicts the execution costs (i.e., execution time) of functions. Based on this model, FUNOff further introduces a code analyzer (Section IV-A), an offloading mechanism (Section IV-B), and an offloading strategy (Section IV-C). These components interact with an MEC environment.

More specifically, Algorithm 1 gives the details. It takes the source code of an application and an MEC environment as its input. Here, the MEC environment is modeled as a graph, in which nodes represent computing nodes (including the mobile device and remote servers with different computation capabilities), and edges represent the communication link between two computing nodes (e.g., the data transmission rate and round-trip time). The output of Algorithm 1 is the offloading scheme, which includes the execution location of each function in the call tree. Algorithm 1 includes the following three procedures:

Procedure 1 (Section IV-A): We implement a code analyzer to extract suitable function invocations. First, it builds a call tree. In this tree, the entry is the main() function; each node represents a function; and a directed edge between nodes represents a

TABLE I  
SYMBOL AND DESCRIPTION

Symbol	Description
$Tree_{f_r} = (F, R)$	Call tree beginning at $f_r$ , where $F$ denotes the set of functions, and $R$ denotes the set of call relations between functions
$fSignature_i$	Function signature of $f_i$
$callSeq_i$	Function call path from $f_{main}$ to $f_i$
$r_{i-j} \in R$	Function call from $f_i$ to $f_j$
$U_j$	Soot statement set of $f_i$
$u_j^i$	$i$ -th soot statement of $U_j$
$N$	Set of computing nodes, including $DS$ , $ES$ , $CS$
$n_k \in N$	Computing node $n_k$
$v_{n_p-n_q}$	Data transmission rate between $n_p$ and $n_q$
$rtt_{n_p-n_q}$	Round-trip time between $n_p$ and $n_q$
$dep(f_i)$	Execution location of $f_i$
$T_{response}$	Response time of application
$T_{dep(f_i)}(f_i)$	Total offloading time of $f_i$
$T_e^{dep(f_i)}(f_i)$	Execution time of $f_i$ in $dep(f_i)$
$T_d^{dep(f_i)}(f_i)$	Data transmission time of $f_i$
$Einvoke_{n_q}^{f_i}$	Execution cost of $f_i$ on $n_q$
$Sinvoke_{n_q}^{f_i}$	Execution cost except external invocations of $f_i$ on $n_q$

function call between two functions (Line 2). Based on the computation complexity and data transmission of each function, it extracts function invocations that are suitable for offloading (Line 3).

Procedure 2 (Section IV-B): We implement an offloading mechanism to enable the remote calls of functions. For the functions extracted in Procedure 1, Line 6 extracts their signatures, and Lines 7 to 11 construct wrappers and transmitters for them according to our program structure.

Procedure 3 (Section IV-C): Based on the results of the above procedures, we design an offloading strategy to determine the offloading scheme according to the context automatically. Different parts of the application can be executed on mobile devices, edge servers, or cloud servers. With this offloading strategy, we implemented an offloading decision algorithm (Algorithm 4). For an application, this algorithm uses the optimization function to calculate the response time of each candidate offloading scheme and selects the scheme with the minimum value.

Table I lists the major symbols used in this paper.

##### A. Code Analyzer

As only a few function calls are suitable for offloading, we employ a preprocessing step, i.e., a program analysis technique for computing offloading. We extract a call tree through static analysis (Section IV-A1). After that, we identify the function invocations suitable for offloading (Section IV-A2) to reduce the additional execution cost of the offloading mechanism and the time cost caused by the decision of offloading schemes.

1) *Extracting the Call Tree*: FUNOff builds a call tree for an object-oriented application. The definition of the call tree is as follows:

*Definition 1.*  $Tree_{f_r} = (F, R)$  denotes a call tree beginning at  $f_r$ , where  $F = \{f_1, f_2, \dots, f_n\}$  is the set of function call sites,

**Algorithm 1:** The Overview of FUNOff.

---

**Input:** The source code of an application *code*; A context environment  $G_c = (N, E)$

**Output:** the offloading scheme  $(DEP)_{optimal} = \{dep(f_1), \dots, dep(f_n)\}$  and the response time  $(T_{response})_{optimal}$

- 1: **procedure** 1
- 2:  $Tree_{f_{main}} = (F, R) \leftarrow$  Algorithm 2(*code*)
- 3:  $divFunction = \{f_1, f_2, \dots, f_p\} \leftarrow$  Algorithm 3( $Tree_{f_{main}}$ )
- 4: **end procedure**
- 5: **procedure** 2
- 6: organize *divFunction* as *DF*
- 7: **for** each  $df_i \in DF$  **do**
- 8:    $Param_i \leftarrow$  collect external parameters of  $df_i$
- 9:    $df_i\_Wrapper \leftarrow$  refactor  $df_i$  with  $Param_i$
- 10:    $df_i\_Transmitter \leftarrow$  refactor  $df_i$
- 11: **end for**
- 12: **end procedure**
- 13: **procedure** 3
- 14:    $\langle (DEP)_{optimal}, (T_{response})_{optimal} \rangle \leftarrow$  Algorithm 4( $Tree_{f_{main}}, G_c, Sinvoke$ )
- 15: **end procedure**

---

**Algorithm 2:** Extracting the Call Tree.

---

**Input:** A  $f_{main}$  function whose statements are  $\{u_{main}^1, \dots, u_{main}^n\}$

**Output:** A call tree  $Tree_{f_{main}} = (F, R)$

- 1:  $F \leftarrow F + f_{main}, R \leftarrow \emptyset$
- 2: **function** *getTree* $f_a, U_a$
- 3: **for** each  $u_a^i \in U_a$  **do**
- 4:    $keywords \leftarrow Soot(u_a^i)$
- 5:   **if**  $\exists "invoke" \in keywords$  **then**
- 6:      $fSignature \leftarrow getfunction(u_a^i)$
- 7:      $callSeq \leftarrow f_a.callSeq + fSignature$
- 8:      $f_s \leftarrow \langle fSignature, callSeq \rangle$
- 9:      $U_s \leftarrow getUnits(fSignature)$
- 10:     $F \leftarrow F + f_s$
- 11:    **if**  $\langle f_a, f_s \rangle \in R.key$  **then**
- 12:       $+ r_{f_a-f_s}$
- 13:    **else**
- 14:       $r_{f_a-f_s} \leftarrow 1$
- 15:       $R \leftarrow R + r_{f_a-f_s}$
- 16:    **end if**
- 17:     $getTree(f_s, U_s)$
- 18:   **end if**
- 19: **end for**
- 20: **end Function**

---

and  $R$  is the set of function call relations. Each edge  $r_{i-j} \in R$  represents a function call from  $f_i$  to  $f_j$ , and its weight represents the call times of the function call.

335   **Definition**           2.  $f_i = \langle fSignature_i, callSeq_i \rangle, f_i \in F$ :  
336    *fSignature<sub>i</sub>* denotes function signature of  $f_i$ , and *callSeq<sub>i</sub>*

TABLE II  
FACTORS FOR IDENTIFYING CUT-POINT FUNCTIONS

Symbol	Description
$\lambda$	Performance ratio between the remote computing node and the local computing node
$v$	Transmission rate between the remote computing node and the local computing node
$rtt$	Round-trip time between the remote computing node and the local computing node

denotes a function call path from the main() function (denoted as  $f_{main}$ , the same below) to  $f_i$ .  
340

FUNOff uses Soot<sup>1</sup> to build call trees, and Algorithm 2 shows  
341 its details. It takes  $f_{main}$  as the entry of the application, and  
342 extracts the call tree beginning at  $f_{main}$ . We get a hash map to  
343 record  $R$ , whose keys are stored in the form of  $\langle f_i, f_j \rangle$ , and  
344 its corresponding value means the times of the call from  $f_i$   
345 to  $f_j$ . The inputs of Algorithm 2 are the entry function  $f_{main}$   
346 and its soot statement set  $U_{main}$ , each  $u_{main}^i$  denotes the  $i$ th  
347 soot statement of  $U_{main}$ . Lines 3 to 20 extract the call tree  
348 recursively via the function *getTree()*, its parameters  $f_a$  denotes  
349 the function to be analyzed, and  $U_a$  denotes  $f_a$ 's soot statements.  
350 In particular, Line 4 obtains the soot keywords in  $u_a^i$ , which is the  
351 instructions defined in Soot. For example, the *invoke* keyword  
352 indicates a function call statement. The complete keywords are  
353 defined in the Soot manual<sup>1</sup>. Therefore, if  $u_a^i$  contains a keyword  
354 that indicates a call to function  $f_s$ , Lines 6 to 10 update  $F$ , that  
355 is, add  $f_s$  to set  $F$ . Lines 11 to 16 update  $R$ , that is, record  
356 the function call from  $f_a$  to  $f_s$  and update its corresponding  
357 value. Line 17 recursively calls the function *getTree()* with  $f_s$   
358 and its statement set. When the procedure is done, the call tree  
359 is obtained.  
360

2) *Extracting Cut-Point Functions:* According to the call tree  
361 extracted in Section IV-A1, FUNOff further identifies function  
362 invocations that are suitable for offloading. For the convenience  
363 of description, we call such function invocations cut-point func-  
364 tions. Table II shows the factors that are collected to identify  
365 cut-point functions. We estimate the performance ratio between  
366 the computing nodes according to the ratio of the time required  
367 to process a set of identical functions on these nodes. The  
368 estimation model of AndroidOff [23] is able to predict the  
369 execution costs of all functions. Following its definition, we  
370 use  $Einvoke_{n_q}^{f_i} = \langle Etime, Edatasize \rangle$  to denote the execution  
371 cost of function  $f_i$  at the computing node  $n_q$ , where *Etime*  
372 denotes the execution time, and *Edatasize* denotes the amount  
373 of data transmission.  
374

For each branch path with the current node as the starting  
375 node, get all nodes on the path from the current node to the first  
376 branch node, and FUNOff chooses the cutpoint functions from  
377 them.  
378

In particular,  $Tree_{f_{cur}}$  denotes the subtree rooted at the  
379 function  $f_{cur}$  of the call tree, and  $T^{Tree_{f_{cur}}}$  denotes the response  
380 time of its local execution.  $T^{Tree_{f_{cur}}}(f_i)$  denotes the response  
381 time of function  $f_i$  in the subtree rooted at  $f_{cur}$ .

<sup>1</sup><https://soot-build.cs.uni-paderborn.de/public/origin/develop/soot/soot-develop/jdoc/>

time of  $Tree_{f_{cur}}$  on the  $f_i$  function call and is calculated as the (1). If  $f_i$  is identified as a cut-point function, all the functions in the subtree rooted at  $f_i$  can be executed on a remote computing node. The response time consists of the local execution time, the remote execution time, and the data transmission time.

Eq. (2) denotes the local execution time, which is calculated as the difference between the total execution time of  $f_{cur}$  and that of  $f_i$  on the local computing node. In particular,  $r_{f_i.caller-f_i}$  denotes the call times of  $f_i$  in a function call to  $f_{cur}$ , it calculates as the product of weight on the path from  $f_{cur}$  to  $f_i$ .

Eq. (3) denotes the remote execution time, which is quantified by the execution cost on a remote computing node over that of a local one.

Eq. (4) denotes the total data transmission time. It consists of the transmission time and the round-trip time. In particular, the transmission time is the amount of data transmission of the cut-point function divided by the transmission rate between the remote computing node and the local computing node, and the round-trip time between two computing nodes is represented as  $rtt$ .

FUNOff extracts cut-point functions based on the above rules and equations. Algorithm 3 describes the details, where the input is the call tree  $Tree_{f_{cur}}$  of the program, and the output is the set of cut-point functions  $divFunction$ . Line 1 sets the  $divFunction$  to the empty set. Then, Line 2 takes  $f_{main}$  as the current function  $f_{cur}$  of the call tree and uses the  $GetDivFunction()$  function to get the  $divFunction$  recursively. Lines 3 to 23 of Algorithm 3 describe the details of the  $GetDivfunction()$ . Line 4 checks whether  $f_{cur}$  has a successor. If it has, Lines 5 to 21 do the following operations on each branch: Lines 7 to 8 add the functions on this branch path to the set  $P$  in order until the first branch node is found. If it exists, line 10 takes it as the current function and recursively calls  $GetDivFunction()$ . Lines 14 to 15 iterate through the functions in  $P$  in turn until a function  $f_i$  is found, so that the response time of  $Tree_{f_{cur}}$  on the  $f_i$  function call is less than the time of local execution. After that, lines 16 to 17 add  $f_i$  to  $divFunction$ , and call the function  $GetDivFunction()$  recursively. When Algorithm 3 is done, a set of all cut-point functions is obtained.

Under the MEC environments with various computational resources and network connections, there might be different numbers of functions that are suitable to be offloaded. Basically, the offloading tends to happen when the higher performance ratio ( $\lambda$ ) between servers and IoT devices and faster data transmission rate ( $v$  and  $rtt$ ). In practical applications, we select the

---

**Algorithm 3:** Extracting Cut-Point Functions.

---

**Input:** A call tree  $Tree_{f_{main}} = (F, R)$   
**Output:** A set of cut-point functions  
 $divFunction = \{f_1, f_2, \dots, f_n\}$   
1:  $divFunction \leftarrow \emptyset$   
2:  $getDivfunction(f_{main})$   
3: **function**  $getDivfunction_{f_{cur}}$   
4: **if**  $post(f_{cur}) \neq \emptyset$  **then**  
5:   **for** each branch path **do**  
6:      $P \leftarrow \emptyset$   
7:     **for** each  $f_i$  in this branch path except  $f_{cur}$  **do**  
8:        $P \leftarrow P \cup f_i$   
9:       **if**  $f_i$  is a branch node **then**  
10:           $getDivfunction(f_i)$   
11:          **break**  
12:       **end if**  
13:     **end for**  
14:     **for** each  $f_i$  in  $P$  **do**  
15:       **if**  $T^{Tree_{f_{cur}}}(f_i) < T^{Tree_{f_{cur}}}$  **then**  
16:           $divFunction \leftarrow divFunction \cup f_i$   
17:           $getDivfunction(f_i)$   
18:          **break**  
19:       **end if**  
20:     **end for**  
21:   **end for**  
22: **end if**  
23: **end Function**

---

429 performance ratio, network transmission rate, and round-trip  
430 time between the remote and the local computing nodes of the  
431 optimal offloading environment in the current scenario as  $\lambda$ ,  
432  $v$ , and  $rtt$  to avoid missing the necessary cut-point functions.  
433 With these factors, the optimization function extracts cut-point  
434 functions that are suitable for offloading and deploying them to  
435 different computing nodes.

436 In an offloading problem, the decision time of offloading  
437 strategy is linearly positive to the number of functions in an  
438 application, and finding the cut-point functions in advance can  
439 effectively reduce the decision time.

### B. Offloading Mechanism

440 A standalone application typically is designed to execute on  
441 only a mobile device. To enable its offloading, FUNOff modifies  
442

$$T^{Tree_{f_{cur}}}(f_i) = T_e^{Tree_{f_{cur}}}(f_i)[local] + T_e^{Tree_{f_{cur}}}(f_i)[remote] + T_d^{Tree_{f_{cur}}}(f_i) \quad (1)$$

$$T_e^{Tree_{f_{cur}}}(f_i)[local] = Einvoke_{n_{cur}}^{f_{cur}}.Etime - Einvoke_{n_{cur}}^{f_i}.Etime * r_{f_i.caller-f_i} \quad (2)$$

$$T_e^{Tree_{f_{cur}}}(f_i)[remote] = \frac{Einvoke_{n_{cur}}^{f_i}.Etime * r_{f_i.caller-f_i}}{\lambda} \quad (3)$$

$$T_d^{Tree_{f_{cur}}}(f_i) = \left( \frac{Einvoke_{n_{cur}}^{f_i}.Edatasize}{v} + rtt \right) * r_{f_i.caller-f_i}. \quad (4)$$

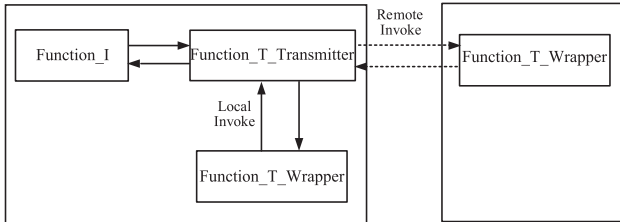


Fig. 4. Target program structure.

```

1: void function (int a, int b) {
2:     d = a +b +c;
3:     return null;
4: }
```

(a) The source code

```

1: Result function (Params params, int a, int b) {
2:     params.d = a +b + params.c;
3:     Result result = new Result();
4:     result.params = params;
5:     result.val = null;
6:     return result;
7: }

Params {
    int c,d; //External variables
}

Result {
    Params params; //Additional return value
    Object val; //Original return value
}
```

(b) The target code of function wrapper

Fig. 5. Example of original function and function wrapper, where  $c$  and  $d$  were external variables (a) The source code. (b) The target code of function wrapper.

443 the source files of applications. To keep program behaviors un-  
444 changed, FUNOff builds wrappers for stateless functions. When  
445 offloading, all the objects of the application are maintained  
446 locally, and parts of function calls are executed remotely; thus,  
447 the application runs normally when the network connection is  
448 changing. This section introduces our target program structure  
449 that supports computation offloading and its refactoring mech-  
450 anism (Section IV-B1), mainly including two parts: function  
451 wrappers (Section IV-B2) and transmitters (Section IV-B3).

452 1) *Target Program Structure*: Our target program  
453 structure is composed of two elements: function wrapper  
454 *Function\_T\_Wrapper* and function transmitter *Func-*  
455 *tion\_T\_Transmitter*, as shown in Fig. 4. In this structure,  
456 an object is deployed locally, and only its function wrappers  
457 are offloaded to a remote server. To enable executing function  
458 wrappers on remote servers, we found their external variables  
459 via static analysis and modified them to be passed in by  
460 parameters and returned by return values. Here, variables  
461 external to the function are those accessed within it but declared  
462 outside. For example, as shown in Fig. 5,  $c$  and  $d$  are the external  
463 variables of the original function.

464 The translation to target programs has three steps:

- 1) Converting function calls from *Function\_I* to *Function\_T* 465 into indirect calls via *Function\_T\_Transmitter*. 466
- 2) Transforming the inputs and the outputs of *Function\_T* to 467 those of *Function\_T\_Wrapper*. As transformed functions 468 don't access external variables, they are stateless. 469
- 3) Generating proxy functions *Function\_T\_Transmitter* for 470 *Function\_T*. *Function\_T\_Transmitter* has the same func- 471 tion signature as *Function\_T*, and it is responsible for de- 472 termining the execution location of *Function\_T\_Wrapper*. 473

474 After the above translation, *Function\_I* calls *Function\_T\_Transmitter* 475 locally, and *Function\_T\_Transmitter* decides whether to call *Function\_T\_Wrapper* 476 locally or remotely according to the offloading decision scheme. The call sites of 477 *Function\_I* to *Function\_T* are unchanged. We next introduce 478 the process of generating function wrappers (Section IV-B2) 479 and function transmitters (Section IV-B3). 480

481 2) *Function Wrapper*: FUNOff generates function wrappers 482 with three steps:

- 1) Modifying the parameters and return values of a function. 483 As shown in Line 1 of Fig. 5(a) and (b), the parameter 484 *params* is added to the original function signature, and 485 it records the external variables of the original function. 486 Through this parameter, external variables are passed into 487 the modified function. In addition, the function in Fig. 5(b) 488 is added to return the values of *params*, so the changes 489 on external variables can be returned to function callers. 490
- 2) Modifying all statements in the function that access exter- 491 nal variables. As shown in Line 2 of Fig. 5(a),  $c$  and  $d$  are 492 two external variables, and as shown in Line 2 of Fig. 5(b), 493 the two external variables are replaced with *params.c* and 494 *params.d*. After the modification, the modified function 495 does not access external variables. 496
- 3) Modifying all return statements for the function. The 497 return statement of Fig. 5(a) is modified to Lines 3 to 6 498 of Fig. 5(b). In particular, *params* is added to the return 499 result, so both the changes in external variables and the 500 return value are returned to function callers. 501

502 3) *Function Transmitter*: A function transmitter is the proxy 503 of a function, which is responsible for handling control mes- 504 sages and data synchronization. The construction of the function 505 transmitter includes the following steps:

- 1) Generating a function whose name, parameters, and return 506 values are identical to the original function, as shown in 507 Line 1 of Fig. 6(b).
- 2) Adding a statement to record the current function call. 508 FUNOff uses a global variable, called *seq*, to represent 509 the position of the current function call in the call tree. As 510 shown in Line 2 of Fig. 6(b), when calling each a function, 511 FUNOff adds its signature to *seq* to record the position of 512 a new function call in the call tree, and as shown in Line 513 15 of Fig. 6(b), it removes the function signature from *seq* 514 when exiting it.
- 3) Adding a statement to handle additional variables. As 515 shown in Lines 3 to 5 of Fig. 6(b), a variable of type 516 *Params* are declared and initialized with the information 517 of local external variables.

```

1: void function (int a, int b) {
2:     d = a +b +c;
3:     return null;
4: }

```

(a) The source code

```

1: Void function (int a, int b) {
2:     seq += function.signature;
3:     Params params = new Params();
4:     params.c = c;
5:     params.d = d;
6:     loc = getloc(seq);
7:     Result result = new Result();
8:     if (loc == Local) {
9:         result = function (params, a, b);
10:    } else {
11:        result = remote(seq, params, a, b);
12:    }
13:    c = result.params.c;
14:    d = result.params.d;
15:    seq -= function.signature;
16:    return result.val;
17: }

```

(b) The target code of function transmitter

Fig. 6. Example of original function and function transmitter, where  $c$  and  $d$  were external variables (a) The source code. (b) The target code of function transmitter.

- 521 4) Adding a statement for the local or remote call to the  
 522 function wrapper. As shown in Lines 6 to 12 of Fig. 6(b),  
 523 FUNOff checks the execution location of the current func-  
 524 tion call in our offloading scheme (Section IV-C1) with  
 525  $seq$  and calls the local function wrapper or the remote  
 526 one. In particular, if a function wrapper is called remotely,  
 527 its parameters and  $seq$  are sent to the agent on the remote  
 528 node, and the remote agent identifies the current function  
 529 call through  $seq$  and invokes it.  
 530 5) Adding the statement to receive the result returned by the  
 531 function wrapper. As shown in Lines 13 to 14 of Fig. 6(b),  
 532 the local external variables are updated with the result data  
 533 to ensure the consistency of program states. In addition,  
 534 the latest return value is returned to its caller, as shown in  
 535 Line 16 of Fig. 6(b).

### C. Offloading Strategy

In this section, we introduce our offloading strategy. It is designed to minimize the overall offloading cost. We next present

the factors that affect the offloading decision (Section IV-C1), the optimization function of our offloading strategy (Section IV-C2), and our offloading decision algorithm to determine the offloading scheme (Section IV-C3).

*1) Contribution Factor:* Offloading schemes determine which functions shall be offloaded and which computing node shall be offloaded. For a given context, it would lead to less overall cost of offloading by using a better offloading scheme. A context contains devices at different scenarios (DS), edge servers (ES), and a cloud server (CS):

*Definition 3.* A context is a graph  $G_C = (N, E)$  representing the network environment, where  $N$  denotes a set of local devices and remote servers, and  $E$  denotes a set of communication links among nodes. Each edge  $(n_p, n_q) \in E$  denotes a data transmission whose rate is  $v_{n_p - n_q}$  and whose round-trip time  $rtt_{n_p - n_q}$  is between  $n_p$  and  $n_q$ .

*Definition 4.* An offloading scheme is defined as  $DEP = \{dep(f_1), dep(f_2), \dots, dep(f_n)\}$ , where  $f_i$  is a function, and  $dep(f_i) \in N$  denotes the computing node to offload the function.

Let  $T_{dep(f_j)}^{dep(f_j)}(f_i)$  represents the total offloading time of  $f_i$ , where  $dep(f_i)$  and  $dep(f_j)$  denote the offloading positions of  $f_i$  and its caller  $f_j$ . The response time of application be expressed as  $T_{response}$ , which equals to the sum of  $T_{dep(f_i)}^{dep(f_j)}(f_i)$ ,  $f_i \in Tree_{f_{main}}.F$ . In addition,  $Sinvoke_{n_q}^{f_i} = \langle Stime, Sdatasize \rangle$  is obtained from the estimation model built in AndroidOff [23], where  $Stime$  denotes the execution time and  $Sdatasize$  denotes the amount of data transmission except external invocations in  $f_i$  executed in  $n_q$ . Note that,  $Einvoke$  mentioned in Section IV-A2 is different from  $Sinvoke$  in that it contains external invocations shown at the bottom of this page.

*2) Optimization Function:* This section introduces our optimization function (5), and we consider the one with the smallest value as the optimal offloading scheme.

Eq. (5) calculates the response time of  $Tree_{f_a}$  (the subtree rooted at  $f_a$ ), which consists of the total offloading time  $T_{dep(f_i)}^{dep(f_j)}(f_i)$  of all functions in this subtree. When  $f_a$  is the  $f_{main}$ , (5) calculates the response time of the application. Algorithm 4 uses it to calculate the response time.

Eq. (6) calculates the total offloading time of  $f_i$ , which is composed of the total execution time  $T_e^{dep(f_i)}(f_i)$  and the total data transmission time  $T_d^{dep(f_i)}(f_i)$  of  $f_i$  in  $dep(f_i)$ .

$$\begin{aligned}
 T_{response}^{f_a} &= T(Sinvoke, G_c, Tree_{f_a}, DEP_{f_a}) \\
 &= \sum_{i=1}^n T_{dep(f_j)}^{dep(f_i)}(f_i), f_i \in Tree_{f_a}.F, \langle f_j, f_i \rangle \in Tree_{f_a}.R.key
 \end{aligned} \tag{5}$$

$$T_{dep(f_j)}^{dep(f_i)}(f_i) = T_e^{dep(f_i)}(f_i) + T_d^{dep(f_i)}(f_i) \tag{6}$$

$$T_e^{dep(f_i)}(f_i) = Sinvoke_{dep(f_i)}^{f_i}.Stime * r_{f_j - f_i} \tag{7}$$

$$T_d^{dep(f_i)}(f_i) = \left( \frac{Sinvoke_{dep(f_i)}^{f_i}.Sdatasize}{v_{dep(f_j) - dep(f_i)}} + rtt_{dep(f_j) - dep(f_i)} \right) * r_{f_j - f_i}. \tag{8}$$

Eq. (7) calculates the total execution time of  $f_i$ , which is the product of  $Stime$  of  $f_i$  in  $dep(f_i)$  and its call times.

Eq. (8) calculates the total data transmission time between  $f_i$  and  $f_j$ , which is the sum of the transmission time and the round-trip time. In particular, the transmission time is calculated as the data transmission amount of  $f_i$  over the transmission rate of  $dep(f_i)$  and  $dep(f_j)$ .

3) *Offloading Decision Algorithm*: A backtracking algorithm [37] transforms the solution space of a problem into a graph or a tree, which finds the optimal one by enumerating all feasible solutions. Based on the backtracking algorithm [37], we propose an offloading decision algorithm for the call-and-return applications. In a call-and-return application, when a function  $A$  calls a function  $B$ , the result returns to  $A$  after  $B$  is executed. For each function, our algorithm explores its execution locations by traversing the call tree in the depth-first order. The algorithm calculates the optimization-function value of each scheme and selects the scheme with the minimum value. Meanwhile, the algorithm integrates the depth-first traversal with the following two pruning mechanisms:

- 1) *Mechanism 1*. A function can be offloaded only if its execution time would be shorter on the offloaded computing node. That is, if a function is executed on the computing node  $A$  and its caller function in the call tree is executed on the computing node  $B$ , the execution time on  $A$  must be shorter than that on  $B$ . Therefore, if there are more available computing nodes, this mechanism tends to reduce more time cost.
- 2) *Mechanism 2*. When the computing node for the function  $f_a$  is determined, the offloading schemes of its subtrees can be decided separately, which are rooted at  $f_a$ 's callee functions in the call tree. Therefore, this mechanism is able to reduce time cost when a call tree has many branches.

Mechanism 1 can effectively offload functions in most cases. As required by this mechanism, a function can only be offloaded to a remote computing node that outperforms the execution result on the local computing node, because it causes extra data transmission time.

For Mechanism 2, the explanation is given as follows: If a call tree  $Tree_{f_a}$  (rooted at  $f_a$ ) contains  $n$  subtrees  $\{Tree_{f_1}, \dots, Tree_{f_n}\}$  and  $Tree_{f_i}$  is a subtree rooted at function  $f_i$ , according to (5), the response time of  $Tree_{f_a}$  is calculated by (9). When the offloading location of  $f_a$ , i.e.,  $dep(f_a)$ , is determined,  $T_{dep(f_a.caller)}^{dep(f_a)}(f_a)$  is a constant. Meanwhile,  $Sinvoke, G_c, Tree_{f_a}, Tree_{f_1}, \dots, Tree_{f_n}$  are fixed parameters, and  $DEP_{f_1}, DEP_{f_2}, \dots, DEP_{f_n}$  are mutually independent parameters. Thus, the minimum response time of  $Tree_{f_a}$  can be calculated by (10), and the offloading schemes of  $f_a$ 's subtrees can be decided separately.

Algorithm 4 describes the decision-making process. For a given call tree  $Tree_{f_{main}}$ , the algorithm searches for the optimal offloading scheme  $DEP_{f_{main}}$  (rooted at  $f_{main}$ ) in a MEC environment  $G_c$ . Line 1 initially adds a virtual function (denoted by  $f_{main.caller}$ ) to  $Tree_{f_{main}}$  and sets the execution locations of  $f_{main}$  and  $f_{main.caller}$  to the mobile device (DS). Line 2 traverses with the function  $getTraversalDEP()$  to obtain  $DEP_{f_{main}}$ . Lines 3 to 32 define the function  $getTraversalDEP()$  that searches for the optimal offloading scheme for the tree or subtree  $Tree_{f_{cur}}$  (rooted at  $f_{cur}$ ), which owns the minimum value of optimization function. Line 4 uses  $DEP_{best}$  to record the best offloading scheme for  $Tree_{f_{cur}}$ . Lines 5 to 6 initialize  $DEP_{best}$  and calculate its value of optimization function  $T_{best}$ , in which execution locations of all functions are set to the one of the caller function  $f_{cur.caller}$ . Line 7 determines whether the computing node for the caller function  $f_{cur.caller}$  perform best: If yes, according to Mechanism 1, all functions in  $Tree_{f_{cur}}$  should be executed at the same computing node as  $f_{cur.caller}$ , and then Line 8 returns the initial scheme of  $DEP_{best}$  and corresponding  $T_{best}$ ; If no, Lines 9 to 31 search for  $DEP_{best}$  by depth-first traversal. Lines 10 to 15 generate candidate computing nodes for executing  $f_{cur}$ , which are recorded in the set  $NodesSet$ . Only cut-point functions can be offloaded, and we determine whether  $f_{cur}$  is a cut-point function: If no,  $NodesSet$  only contains the computing node for the caller function  $dep(f_{cur.caller})$ ; If yes,  $NodesSet$  also contains computing nodes with better performance than

$$\begin{aligned} T_{response}^{f_a} &= T(Sinvoke, G_c, Tree_{f_a}, DEP_{f_a}) \\ &= T_{dep(f_a.caller)}^{dep(f_a)}(f_a) + T_{response}^{f_1} + T_{response}^{f_2} + \dots + T_{response}^{f_n} \\ &= T_{dep(f_a.caller)}^{dep(f_a)}(f_a) + T(Sinvoke, G_c, Tree_{f_1}, DEP_{f_1}) + T(Sinvoke, G_c, Tree_{f_s}, DEP_{f_s}) \\ &\quad + \dots + T(Sinvoke, G_c, Tree_{f_n}, DEP_{f_n}) \end{aligned} \tag{9}$$

$$\begin{aligned} \min(T_{response}^{f_a}) &= \min(T_{dep(f_a.caller)}^{dep(f_a)}(f_a) + T_{response}^{f_1} + T_{response}^{f_2} + \dots + T_{response}^{f_n}) \\ &= \min(T_{dep(f_a.caller)}^{dep(f_a)}(f_a) + T(Sinvoke, G_c, Tree_{f_1}, DEP_{f_1}) + T(Sinvoke, G_c, Tree_{f_s}, DEP_{f_s}) \\ &\quad + \dots + T(Sinvoke, G_c, Tree_{f_n}, DEP_{f_n})) \\ &= \min(T_{dep(f_a.caller)}^{dep(f_a)}(f_a)) + \min(T(Sinvoke, G_c, Tree_{f_1}, DEP_{f_1})) + \min(T(Sinvoke, G_c, Tree_{f_s}, DEP_{f_s})) \\ &\quad + \dots + \min(T(Sinvoke, G_c, Tree_{f_n}, DEP_{f_n})). \end{aligned} \tag{10}$$

**Algorithm 4:** Offloading Decision Algorithm.

---

**Input:** A call tree  $Tree_{f_{main}} = (F, R)$ ; a context environment  $G_c = (N, E)$ ; a set of execution costs for each function except external invocations  $Sinvoke$

**Output:** An offloading scheme  $DEP_{f_{main}} = \{dep(f_1), dep(f_2), \dots, dep(f_n)\}$ ; the response time  $T_{response}$

```

1:  $DEP_{f_{main}}.dep(f_{main}), DEP_{f_{main}}.dep(f_{main.caller}) \leftarrow DS$ 
2:  $DEP_{f_{main}}, T_{response} \leftarrow getTraversalDEP(f_{main}, DEP_{f_{main}}.dep(f_{main.caller}))$ 
3: function  $getTraversalDEP(f_{cur}, dep(f_{cur.caller}))$ 
4:    $DEP_{best} \leftarrow DEP_{f_{cur}}$ 
5:    $DEP_{best}.dep(f_i) \leftarrow dep(f_{cur.caller}), \forall f_i \in Tree_{best}$ 
6:    $T_{best} \leftarrow \text{optimization function}(Sinvoke, G_c, Tree_{f_{cur}}, DEP_{best})$ 
7:   if  $dep(f_{cur.caller})$  is the best performing computing node then
8:     return  $DEP_{best}, T_{best}$ 
9:   else
10:     $NodesSet \leftarrow \emptyset, NodesSet \leftarrow NodesSet + dep(f_{cur.caller})$ 
11:    if  $f_{cur} \in divFunction$  then
12:      for each computing node  $n$  with better performance than  $dep(f_{cur.caller})$  do
13:         $NodesSet \leftarrow NodesSet + n$ 
14:      end for
15:    end if
16:    for each  $n \in NodesSet$  do
17:       $DEP_{temp} \leftarrow DEP_{f_{cur}}$ 
18:       $DEP_{temp}.dep(f_{cur}) \leftarrow n$ 
19:      if  $post(f_{cur}) \neq \emptyset$  then
20:        for each  $f_i$  in  $post(f_{cur})$  do
21:           $DEP, T \leftarrow getTraversalDEP(f_i, n)$ 
22:           $DEP_{temp}.dep(f_j) \leftarrow DEP.dep(f_j), \forall f_j \in Tree_{f_i}$ 
23:        end for
24:      end if
25:       $T_{temp} \leftarrow \text{optimization function}(Sinvoke, G_c, Tree_{f_{cur}}, DEP_{temp})$ 
26:      if  $T_{temp} < T_{best}$  then
27:         $T_{best} \leftarrow T_{temp}, DEP_{best} \leftarrow DEP_{temp}$ 
28:      end if
29:    end for
30:    return  $DEP_{best}, T_{best}$ 
31:  end if
32: end Function

```

---

657  $dep(f_{cur.caller})$ , according to Mechanism 1. Lines 16 to 29  
 658 respectively perform a depth-first traversal of  $Tree_{f_{cur}}$ , for  
 659 each candidate computing node  $n$  for  $f_{cur}$  ( $n \in NodesSet$ ).  
 660 According to Mechanism 2, when the execution location of  
 661  $f_{cur}$  is fixed, the offloading schemes of its subtrees can be  
 662 decided separately, which are rooted at  $f_{cur}$ 's callee functions  
 663 in the call tree. The traversal is as follows: Lines 17 to 18 use  
 664  $DEP_{temp}$  to record the best offloading scheme for  $Tree_{f_{cur}}$   
 665 when the execution location of  $f_{cur}$  is  $n$ . To obtain  $DEP_{temp}$ ,  
 666 Lines 19 to 24 call the function  $getTraversalDEP()$  for  
 667 each  $f_{cur}$ 's callee functions  $f_i$  to obtain the best offloading  
 668 scheme for  $Tree_{f_i}$ . Lines 25 to 28 calculate the optimization-  
 669 function value of  $DEP_{temp}$ , and update  $DEP_{best}$  if it is less  
 670 than the current  $DEP_{best}$ . When the traversal (Lines 16 to 29)  
 671 is completed, Line 30 returns  $DEP_{best}$  and the corresponding  
 672  $T_{best}$ . Based on the function  $getTraversalDEP()$ , the optimal  
 673 offloading scheme  $DEP_{f_{main}}$  can be obtained.

**V. EVALUATION**

In this section, we established an MEC environment to evaluate the effectiveness of FUNOff (Section V-A). In this environment, we compared FUNOff with AndroidOff [23], [24] and MAUI [9] (Section V-B). Beside the overall effectiveness, we conducted experiments to explore the details of FUNOff (Section V-C).

**A. MEC Environment**

Our MEC environment includes two scenes (college and community), and each scene contains four regular locations. In total, our experimental environment uses five computing nodes, including two mobile devices and three remote servers. Table III lists the network conditions between these computing nodes, where each cell denotes the round-trip time and the data transmission rate between our mobile devices and corresponding

TABLE III  
THE DEVICE CONTEXTS

(a) College

	Playground	Teaching building	Garden	Laboratory	Cloud
Edge1	-	RTT = 40ms V = 1.5Mb/s	RTT = 40ms V = 1.5Mb/s	-	RTT = 40ms V = 1.5Mb/s
Edge2	-	-	RTT = 70ms V = 1.0Mb/s	RTT = 40ms V = 1.5Mb/s	RTT = 40ms V = 1.5Mb/s
Cloud	RTT = 200ms V = 200kb/s	RTT = 200ms V = 200kb/s	-	RTT = 70ms V = 1.0Mb/s	-

(b) Community

	Residence	Traffic Road	Parking Lot	Store	Cloud
Edge1	-	RTT = 40ms V = 1.5Mb/s	-	RTT = 60ms V = 1.2Mb/s	RTT = 20ms V = 2Mb/s
Edge2	RTT = 60ms V = 1.2Mb/s	RTT = 70ms V = 1.0Mb/s	-	-	RTT = 20ms V = 2Mb/s
Cloud	RTT = 100ms V = 500kb/s	-			

TABLE IV  
THE PERFORMANCE OF COMPUTING NODES

	Device1	Device2	Edge1	Edge2	Cloud
Performance evaluation	1	1.2	2.2	2.8	4.4

remote servers. For example, in Table III(a), the fourth column of the second row denotes that the round-trip time between our mobile device and Edge1 is 40ms, and the transmission rate reaches 1.5Mb/s in the garden. The data in Table III are collected by WLAN-RTT.<sup>2</sup>

We have installed the applications on two mobile devices. One mobile device is Huawei Honor MYA-AL10<sup>3</sup> with a 1.4 GHz 4 core CPU, 2 GB RAM (Device1, the low-end device) and the other is Huawei Honor STF-AL00<sup>4</sup> with 2.4 GHz 4 core CPU, 4 GB RAM (Device2, the high-end device). Our MEC environment has two edge servers (Edge1 and Edge2) and a cloud server (cloud). Edge1 is a server with a 2.5 GHz 8 core CPU and 4 GB RAM; Edge2 is a server with a 3.0 GHz 8 core CPU and 8 GB RAM; Cloud is a server with a 3.6 GHz 16 core CPU and 16 GB RAM. To measure the performance of each computing node, we execute an identical set of functions, and compare the execution time with that on Device1. Table IV shows the results.

In our evaluations, the subject applications include a License Plate Recognition Application (LPRA) and a Target Detection Application (TDA). LPRA performs preprocessing and ocr processing on the images that are extracted from video frames to obtain the license plate numbers, and stores them on the mobile device. TDA performs pedestrian detection and feature extraction on the images extracted from the video and saves the results on the mobile device after feature comparison with the person to be recognized. We installed them on both mobile devices. In our experiments, we walk around the above two scenes and execute these two applications. In this process, we record the data transmission amount and the execution time of each function call on devices, Edge1, Edge2, and Cloud. Upholding the principle of

rigor, we repeat this process twenty times to avoid unnecessary errors. For example, Fig. 7(a) shows the collected LPRA data on the Huawei Honor MYA-AL10. The ellipse indicates the function, and the data above it indicates the execution time of the function on this device. For example, 16 in the dashed box indicates the time (in ms) of one execution of the function OAlg.gm() on Huawei Honor MYA-AL10. The connecting line indicates the call relationship between the functions, and its data indicates the number of calls and the amount of data transferred between them. For example, 1:280 in the dashed box indicates the function OAlg.Graymath() makes one call to the function OAlg.gm(), and the amount of data transfer generated by one call is 280B. Fig. 7(b) shows the collected TDA data on the Huawei Honor MYA-AL10.

The parameters  $\lambda$ ,  $v$  and  $rtt$  used in the preprocessing algorithm (Algorithm 3) need to be set according to the ideal offloading environment. To find all possible cut-points during the preprocessing phase, the ideal offloading environment in our experimental environments (i.e., from the Huawei Honor MYA-AL10 to the Edge2 in the laboratory of college) is selected with the consideration of server performance and data transmission rate to conduct the simulation offloading experiment of Algorithm 3.  $\lambda$  is set to 2.8 based on the performance ratio between MYA-AL10 and Edge2, as shown in Table IV.  $v$  and  $rtt$  are set to 1.5 Mb/s and 40ms, respectively, based on the network connection between them, as shown in Table III(a).

### B. Overall Comparison

1) *Compared Approach and Scenarios:* In this section, we compared FUNOff with AndroidOff [23], [24] and MAUI [9]. AndroidOff works at the granularity of objects. It traverses all possible deployments from the mobile device to servers, and searches for the decision that can minimize the response time. MAUI works at the granularity of methods. It uses integer linear programming to decide where the movable functions shall be moved to servers.

Owing to the mobility of devices, we considered the following two scenarios: (1) we stay in different fixed locations with mobile devices (Section V-B2) and (2) with mobile devices, we move between different locations in the college and community respectively (Section V-B3). We use the response time generated by the real execution of the application as the metric of performance. In addition to task execution and data transmission time, the response time includes the additional time overhead generated by the mechanisms. Each experiment is repeated for 20 times to ensure its reliability [22].

2) *Performance Comparison of Fixed Locations:* Fig. 8 shows that FUNOff achieves the best performance in all cases. Fig. 9 shows the offloading schemes of AndroidOff, MAUI, and FUNOff when running LPRA on Honor MYA-AL10 in the garden.

Comparing the functions of the RecInEachChar class in Fig. 9(a) with (b) we find that FUNOff offloaded the instances of these functions to three computing nodes (Edge2, Cloud, and Device1). Note that the device can connect to the Cloud via Edge1 or Edge2; AndroidOff offloaded the instances of

<sup>2</sup><https://developer.android.google.cn/guide/topics/connectivity/wifi-rtt>

<sup>3</sup><http://huawei-update.com/device-list/mya-al10>

<sup>4</sup><http://huawei-update.com/device-list/stf-al00>

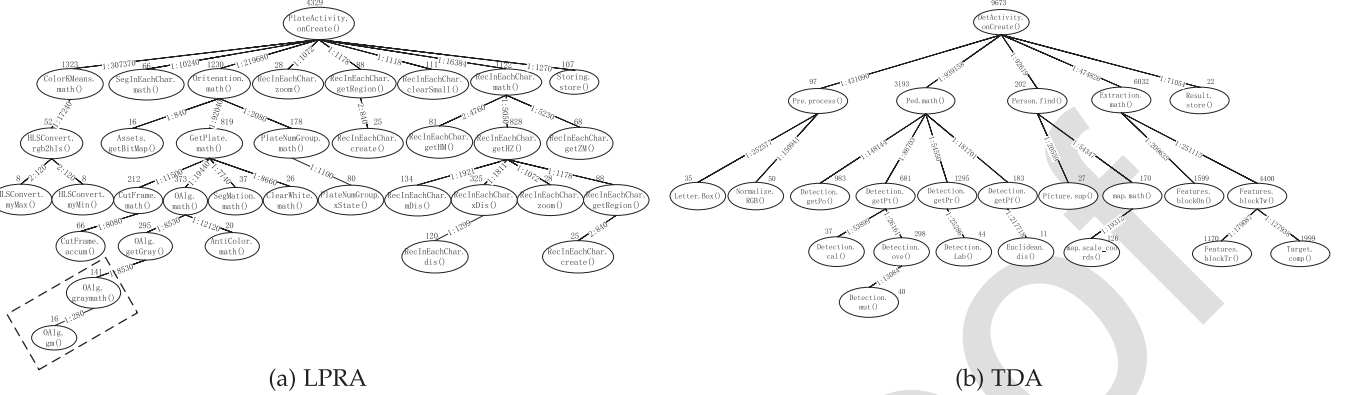


Fig. 7. LPRA and TDA performed on Huawei Honor MYA-AL10 (a) LPRA. (b) TDA.

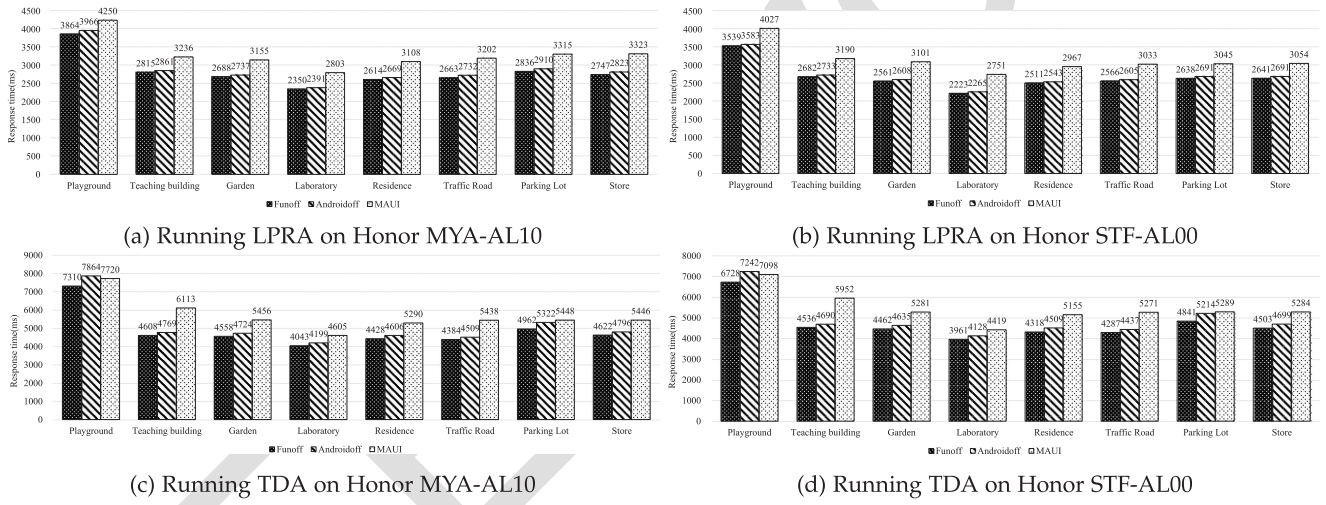


Fig. 8. Performance comparison of running LPRA and TDA with different offloading approaches when staying in different locations fixedly (a) Running LPRA on Honor MYA-AL10. (b) Running LPRA on Honor STF-AL00 (c) Running TDA on Honor MYA-AL10 (d) Running TDA on Honor STF-AL00.

775 the whole class to Edge2. As our offloading granularity is  
776 finer, FUNOff is more flexible than AndroidOff. As a result,  
777 it improves the results of AndroidOff.

778 Comparing Fig. 9(a) with (c), we find that MAUI moved all  
779 methods to a single server, and this scheme is sub-optimized.  
780 Instead, as our offloading decision can weigh the different net-  
781 work connections, FUNOff offloaded the functions whose data  
782 transmission is intensive to remote servers with good network  
783 connections. Meanwhile, as our offloading decision can weigh  
784 the different performance of servers, FUNOff offloaded the  
785 functions whose computation is intensive to remote servers with  
786 better computation power but relatively poor network connec-  
787 tions.

788 To further analyze our improvements, we next introduce the  
789 results of LPRA, when it is installed on Honor MYA-AL10  
790 and moved around the playground. Both FUNOff and MAUI  
791 support offloading at function granularity, and only a cloud  
792 server is available here, so their offloading schemes are the  
793 same. However, the results in Fig. 8(a) show that FUNOff  
794 still improves by about 10% over MAUI. This is because the  
795 offloading mechanism introduces additional overhead such as

the execution of extra statements, the response time of the  
796 server, etc. Since FUNOff only refactors the cut-point functions,  
797 while MAUI needs to refactor all the methods, this causes more  
798 additional overhead. And AndroidOff will incur an overhead of  
799 approximately 170 ms, which originates from the proxies.

800 *3) Performance Comparison When Cruising Between Dif-  
801 ferent Locations:* Due to the different computing resources and  
802 network connections in locations, the offloading scheme needs  
803 to be updated when a mobile device moves to a new location. The  
804 results from Honor MYA-AL10 and Honor STF-AL00 in both  
805 the college and community scenes are consistent. For simplicity,  
806 we only show the results of MYA-AL10 when it is in the college.  
807 Fig. 10 shows the decision and preparation costs in the four  
808 locations of the college scene. According to the results, FUNOff  
809 has the following advantages:

810 (1) FUNOff has the least decision time. For this measure,  
811 the averages of FUNOff, AndroidOff, and MAUI on LPRA are  
812 218ms, 1,206ms, and 442ms, and the averages on TDA are 3.8ms,  
813 1333ms, and 280ms, respectively. FUNOff only decides the  
814 offloading position of cut-point functions, and different branches  
815 can make decisions independently, the details of Algorithm 3 are

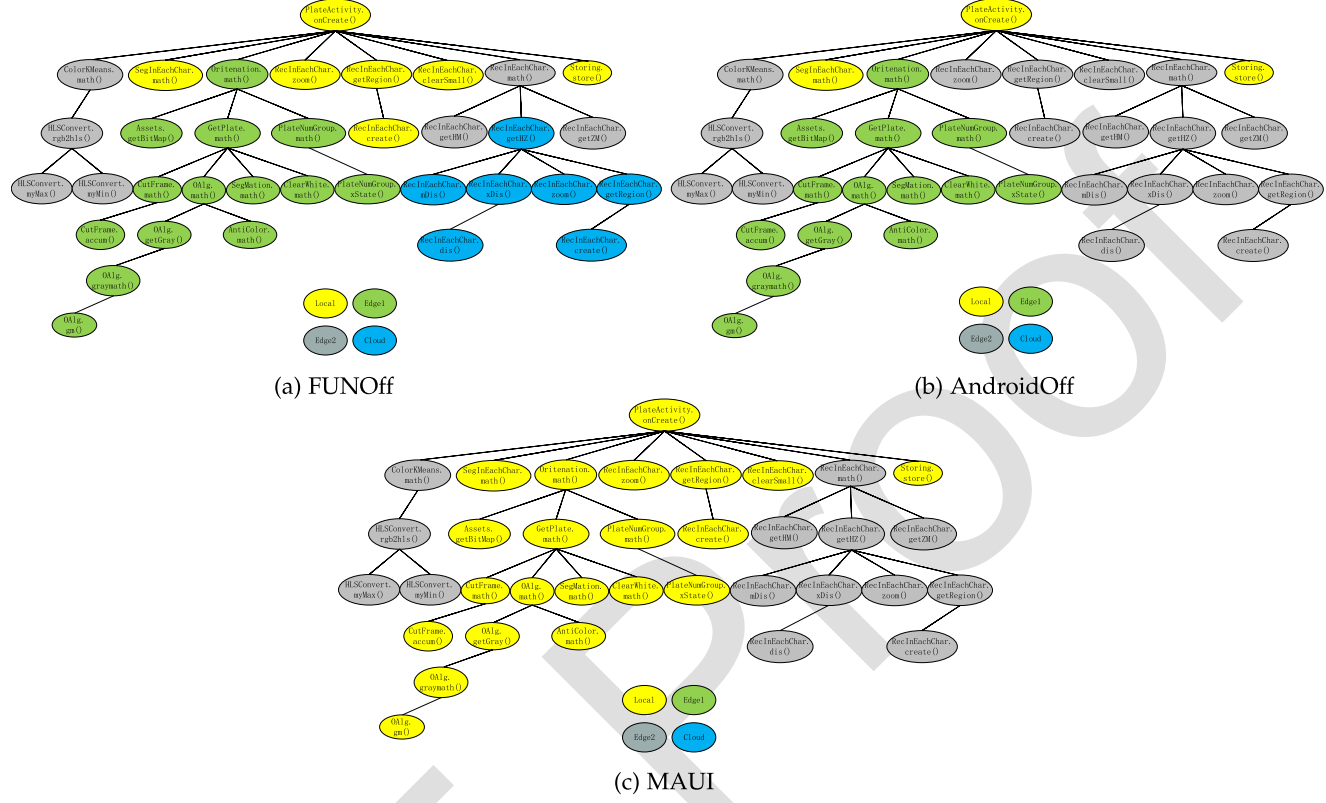


Fig. 9. Offloading schemes when running LPRA on the Honor MYA-AL10 in garden (a) FUNOff. (b) AndroidOff (c) MAUI.

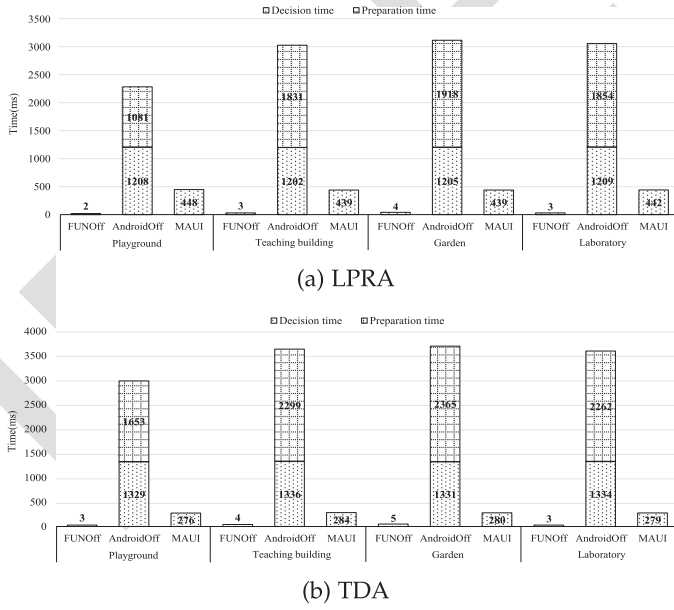


Fig. 10. The time cost of adjusting offloading schemes of different offloading approaches for LPRA and TDA on the Honor MYA-AL10 in the college (a) LPRA. (b) TDA.

shown in Section IV-C3. Therefore, it can make decisions in a short time. AndroidOff is based on traversal and needs to select the best one from all possible object distribution schemes. Therefore, its decision time is exponentially related to the number of

movable objects. MAUI is based on the program partitioning strategy, and determines offloading schemes at runtime. Therefore, its decision time is linearly related to the number of movable methods. The compared approaches require more decision times than FUNOff.

(2) When the network connection changes, FUNOff and MAUI do not need extra preparations for the new compute offloading, but the average preparation time of AndroidOff on LPRA and TDA are 1,671ms and 2145ms, respectively. Both FUNOff and MAUI offload applications at the granularity of functions (methods), and they store program states on mobile devices. As a result, functions can be executed directly on a new remote server when the network connection changes. AndroidOff offloads applications at the granularity of objects, and objects are executed on either mobile devices, edge servers, or cloud servers. When an offloading scheme changes, the application needs to offload the objects from an old computing node to a new computing node. Moreover, if an offloaded object becomes inaccessible, the application crashes and has to be restarted.

Fig. 11 shows results on Honor MYA-AL10. FUNOff has the best results; AndroidOff is the second in most cases; and MAUI has the worst. FUNOff and AndroidOff can use multiple remote servers for computation offloading, but MAUI is designed to use a single remote server. When the device context changes, the response time of FUNOff and MAUI only increases slightly due to the additional cost caused by making decisions. In contrast, the response time of AndroidOff increases by about three seconds, mainly due to the decision time and the offloading

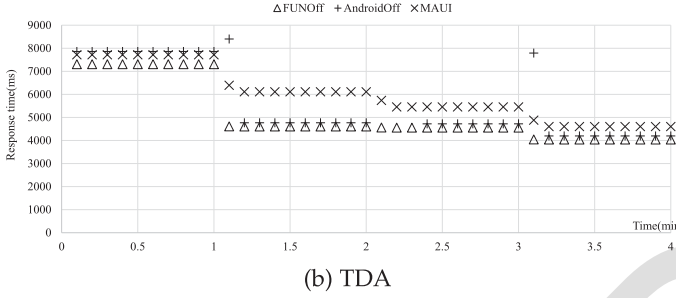
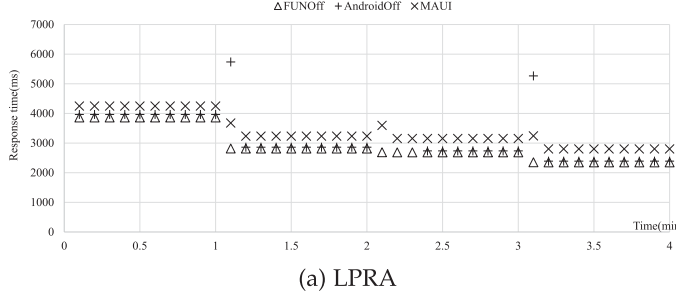


Fig. 11. Performance comparison of running LPRA and TDA on Honor MYA-AL10 with different offloading approaches when cruising between four locations in the college (a) LPRA. (b) TDA.

849 preparation time. In addition, when the device cruised from the  
850 teaching building to the garden, AndroidOff failed to respond  
851 for about twenty seconds. The original object on the cloud was  
852 inaccessible, so the application crashed and restarted.

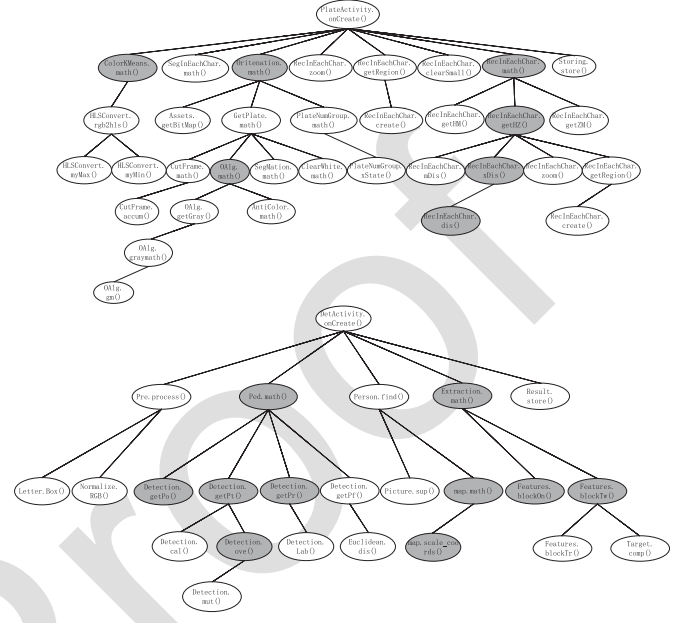
### 853 C. Detailed Comparison

854 In this section, we explore the effectiveness of the cut-point  
855 algorithm (Section V-C1), the offloading schemes of different  
856 decision algorithms (Section V-C2), and their time costs (Sec-  
857 tion V-C3).

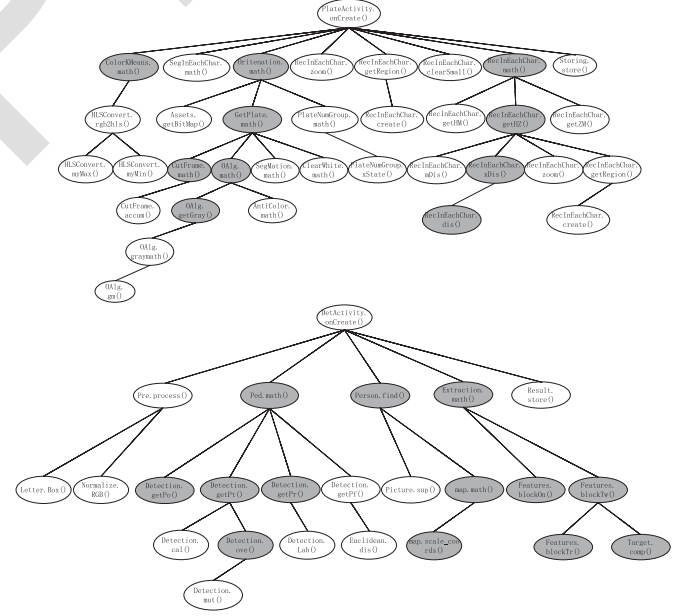
858 *1) Evaluation of the Cut-Point Algorithm: Setting.* In this  
859 section, we evaluate the rationality and feasibility of the cut-  
860 point algorithm (Algorithm 3) which extracts cut-point functions  
861 from the call tree.

862 For each case, we analyze the call tree and the MEC environ-  
863 ment to manually obtain the corresponding optimal offloading  
864 scheme. Next, we take the union of functions offloaded in those  
865 offloading schemes as the ideal set of cut-point functions, i.e., the  
866 gray nodes as shown in Fig. 12(a). We compare the set obtained  
867 by the cut-point algorithm (Algorithm 3) with the ideal set. If the  
868 cut-point set covers the ideal set, our cut-point algorithm can find  
869 all the functions offloaded in those optimal offloading schemes  
870 and will not affect the search for the optimal offloading scheme.  
871 If the cut-point set contains redundant cut-point functions, the  
872 extra number of decisions due to the extra cut-point functions  
873 will incur additional decision overhead. With the parameters set  
874 in Section V-A, we use Algorithm 3 to calculate the cut-point  
875 set, and compare it with the ideal set.

876 *Result.* Fig. 12(b) shows the results of the cut-point algorithm.  
877 Comparing this figure with Fig. 12(a), the ideal set can be  
878 covered by the cut-point set obtained by the cut-point algorithm.  
879 Meanwhile, the additional decision cost caused by the redundant



(a) The ideal set of cut-point functions



(b) The cut-point set obtained by Algorithm 3

Fig. 12. Sets of the cut-point functions of LPRA and TDA (a) The ideal set of cut-point functions. (b) The cut-point set obtained by Algorithm 3.

cut-point functions in our set is acceptable, which will be dis-  
cussed in Section V-C3.

881 *2) Evaluation of the Offloading Decision Algorithm: Setting.*  
882 In this section, we compare our decision algorithms with the  
883 traversal algorithm [23], [24], the Q-learning [38], the particle  
884 swarm optimization with the genetic algorithm (PSO-GA) [31],  
885 and the classical genetic algorithm (GA) [30]. In particular, our  
886 comparison includes two stages: with or without our preproces-  
887 sing step, which extracts cut-point functions.

888 *Traversal Algorithm.* The unpreprocessed traversal algorithm  
889 obtains the optimal offloading scheme by enumerating the com-  
890 binations of all the functions on different computing nodes. The  
891

TABLE V  
RESULTS OF OFFLOADING SCHEMES OBTAINED BY DIFFERENT DECISION ALGORITHMS

(a) LPRA

Device and location	Algorithm	Optimal scheme (Traversal Algorithm Without preprocessing)	Traversal Algorithm			Our Algorithm		Q-learning		PSO-GA		GA	
			With preprocessing	Without preprocessing	With preprocessing	Without preprocessing	With preprocessing	Without preprocessing	With preprocessing	Without preprocessing	With preprocessing	Without preprocessing	With preprocessing
Honor MYA-AL10	College	Playground	3864.4ms	✓	✓	✓	✓	✓	✓	2.947%	0.531%	5.509%	2.531%
		Teaching building	2814.8ms	✓	✓	✓	✓	✓	✓	11.142%	0.508%	21.711%	2.008%
		Garden	2687.7ms	✓	✓	✓	✓	✓	✓	8.896%	0.484%	15.683%	1.838%
		Laboratory	2349.8ms	✓	✓	✓	✓	✓	✓	8.669%	0.813%	13.473%	2.072%
	Community	Residence	2613.9ms	✓	✓	✓	✓	✓	✓	8.195%	0.318%	10.035%	1.546%
		Traffic Road	2662.9ms	✓	✓	✓	✓	✓	✓	5.310%	0.109%	9.001%	0.792%
		Parking Lot	2836.3ms	✓	✓	✓	✓	✓	✓	5.014%	0.328%	8.254%	0.709%
		Store	2747.4ms	✓	✓	✓	✓	✓	✓	7.360%	0.335%	13.340%	1.350%
Honor STF-AL00	College	Playground	3539.1ms	✓	✓	✓	✓	✓	✓	1.138%	0.330%	1.314%	0.554%
		Teaching building	2682.4ms	✓	✓	✓	✓	✓	✓	11.014%	0.933%	18.574%	2.003%
		Garden	2560.8ms	✓	✓	✓	✓	✓	✓	8.218%	0.575%	13.892%	1.556%
		Laboratory	2223.2ms	✓	✓	✓	✓	✓	✓	8.940%	0.817%	13.159%	1.928%
	Community	Residence	2510.7ms	✓	✓	✓	✓	✓	✓	9.053%	0.315%	13.941%	1.386%
		Traffic Road	2565.7ms	✓	✓	✓	✓	✓	✓	6.945%	0.226%	15.208%	0.760%
		Parking Lot	2638.3ms	✓	✓	✓	✓	✓	✓	4.219%	0.023%	12.910%	0.788%
		Store	2640.6ms	✓	✓	✓	✓	✓	✓	7.726%	0.360%	14.364%	1.015%

(b) TDA

Device and location	Algorithm	Optimal scheme (Traversal Algorithm Without preprocessing)	Traversal Algorithm			Our Algorithm		Q-learning		PSO-GA		GA	
			With preprocessing	Without preprocessing	With preprocessing	Without preprocessing	With preprocessing	Without preprocessing	With preprocessing	Without preprocessing	With preprocessing	Without preprocessing	With preprocessing
Honor MYA-AL10	College	Playground	7309.7ms	✓	✓	✓	✓	✓	✓	13.325%	1.316%	17.250%	5.241%
		Teaching building	4608.1ms	✓	✓	✓	✓	✓	✓	26.454%	4.681%	39.778%	11.094%
		Garden	4557.5ms	✓	✓	✓	✓	✓	✓	28.024%	3.291%	41.068%	9.521%
		Laboratory	4042.7ms	✓	✓	✓	✓	✓	✓	32.355%	6.258%	45.972%	15.312%
	Community	Residence	4428.3ms	✓	✓	✓	✓	✓	✓	27.080%	7.023%	39.021%	17.094%
		Traffic Road	4384.4ms	✓	✓	✓	✓	✓	✓	18.943%	7.960%	33.396%	13.274%
		Parking Lot	4962.0ms	✓	✓	✓	✓	✓	✓	25.058%	8.102%	31.929%	14.833%
		Store	4622.5ms	✓	✓	✓	✓	✓	✓	27.636%	7.745%	45.773%	17.977%
Honor STF-AL00	College	Playground	6727.9ms	✓	✓	✓	✓	✓	✓	12.481%	6.416%	15.552%	10.826%
		Teaching building	4536.4ms	✓	✓	✓	✓	✓	✓	23.343%	1.869%	36.925%	11.502%
		Garden	4462.4ms	✓	✓	✓	✓	✓	✓	24.843%	1.791%	37.599%	8.815%
		Laboratory	3961.1ms	✓	✓	✓	✓	✓	✓	24.135%	0.444%	39.863%	7.885%
	Community	Residence	4317.5ms	✓	✓	✓	✓	✓	✓	26.201%	7.736%	40.173%	17.232%
		Traffic Road	4286.7ms	✓	✓	✓	✓	✓	✓	20.065%	5.692%	33.936%	13.390%
		Parking Lot	4841.5ms	✓	✓	✓	✓	✓	✓	17.242%	7.539%	25.426%	11.402%
		Store	4502.5ms	✓	✓	✓	✓	✓	✓	24.566%	8.262%	41.624%	18.301%

892 preprocessed traversal algorithm enumerates only the cut-point  
 893 functions.

894 *Our Algorithms.* We design two versions of Algorithm 4. The  
 895 original version is called the preprocessed decision algorithm,  
 896 which makes decisions for the cut-point functions. Another  
 897 version is called the unpreprocessed decision algorithm, which  
 898 makes decisions on the execution location for all functions of  
 899 the call tree.

900 *Q-Learning.* It stores each state-action pair and its correspond-  
 901 ing Q-values into a Q-table, and maximizes the accumulative  
 902 rewards of an offloading plan. The learning rate  $\alpha$ , the discount  
 903 factor  $\beta$ , the probability of  $\varepsilon$ -greedy, and the max training  
 904 epochs are set to 0.01, 0.95, 0.1, and 100,000, respectively. The  
 905 algorithm will terminate and return the best one when the result  
 906 is constant for 5,000 consecutive iterations. The unpreprocessed  
 907 Q-learning needs to make decisions for all functions, while  
 908 the preprocessed Q-learning only makes decisions for cut-point  
 909 functions.

910 *PSO-GA.* It introduces the crossover and mutation operators  
 911 of GA to improve the particle update strategy of the traditional  
 912 PSO algorithm. The unpreprocessed version encodes all the  
 913 functions into a chromosome, and the preprocessed version only  
 914 encodes the cut-point functions. The start and end values of  
 915 the two acceleration coefficients  $c_1$  and  $c_2$ , and the maximum  
 916 and minimum values of the inertia weight  $w$  are set to 0.9,

917 0.2, 0.9, 0.4, 0.9, and 0.4, respectively. The iteration number  
 918 and population number of the unpreprocessed PSO-GA are set  
 919 to 2000 and 150, while the preprocessed ones are set to 1100  
 920 and 80.

921 GA. The unpreprocessed genetic algorithm encodes all the  
 922 functions into a chromosome, applies genetic operations (e.g.,  
 923 selection, crossover, and mutation) to generate new offloading  
 924 schemes, and uses the optimization function to select the best  
 925 ones. The evolutionary generation, the population number, the  
 926 crossover probability, and the mutation probability are set as  
 927 2,000, 150, 0.6, and 0.3. The preprocessed genetic algorithm  
 928 only encodes the cut-point functions, and its parameters are set  
 929 as 1,100, 80, 0.6, and 0.3, respectively.

930 As the traversal algorithm enumerates all candidate offloading  
 931 schemes, it is able to find the optimal scheme. We take its optimal  
 932 scheme and response time as the baseline. If the response time  
 933 corresponding to the offloading scheme obtained by other algo-  
 934 rithms is consistent with it, it means that they find the optimal  
 935 scheme. If the response time is larger than the baseline, the  
 936 algorithm finds an offloading scheme with a worse performance  
 937 than the optimal scheme, and the larger the response time, the  
 938 worse the performance. Each algorithm is repeated 20 times  
 939 separately and the average value is taken as its final result.

940 *Result.* The experimental results are shown in Table V. The  
 941 tick in this table indicates that the corresponding algorithm

942 finds the optimal offloading scheme. The gray part indicates  
 943 that it does, and the values denote the increased response time  
 944 compared with the optimal offloading scheme. For example,  
 945 in the scenario of Honor MYA-AL10 in the playground in Ta-  
 946 ble V(a), the response time corresponding to the optimal scheme  
 947 is 3864.4ms. In this scenario, the response time corresponding  
 948 to the offloading scheme obtained from the unpreprocessed  
 949 PSO-GA is 3978.3ms, which is an increase of 2.947% compared  
 950 to 3864.4ms, so the value of the corresponding position in  
 951 Table V(a) is set to 2.947%.

952 First, we compare the performance of the algorithms without  
 953 preprocessing. As shown in Table V, our algorithm achieves the  
 954 same performance as the traversal algorithm for all the 32 cases.  
 955 Our algorithm finds the optimal schemes, since it is an improved  
 956 traversal algorithm and its two effective pruning mechanisms are  
 957 unlikely to affect the search for the optimal offloading scheme  
 958 (Section IV-C3 for more details). The Q-learning adaptively  
 959 learns appropriate scheduling decisions by interacting with the  
 960 network environment and can obtain the same results as the  
 961 traversal algorithm in 26 of 32 total cases. However, in other  
 962 6 cases, its response time is 0.319%-4.374% higher than the  
 963 traversal algorithm. Unlike the traversal algorithm that enumera-  
 964 tes all candidate offloading schemes, the learning process of  
 965 Q-learning is uncertain. As the low occurrence of some states  
 966 causes the randomness of the Q-table, Q-learning is unable to  
 967 achieve an optimal offloading scheme in some cases. PSO-GA  
 968 cannot obtain the optimal offloading schemes in all cases, and  
 969 its response time is 1.138%-32.355% more than the optimal  
 970 offloading scheme. Although PSO-GA improves the stochastic-  
 971 ity through the crossover operations, it still suffers from local  
 972 optima. Therefore, PSO-GA fails to obtain the global optimal  
 973 scheme in a large solution space. Similarly, GA cannot obtain  
 974 the optimal offloading schemes in all cases, and its response time  
 975 is 1.314%-45.972% more than the optimal offloading scheme.  
 976 GA has strong stochasticity and converges slowly, and thus it is  
 977 difficult to converge to a better offloading scheme with a limited  
 978 number of iterations.

979 Furthermore, we compare the performance of each algorithm  
 980 with and without preprocessing. The traversal algorithm with  
 981 preprocessing still obtains the optimal scheme in all cases,  
 982 because the cut-point set obtained by the cut-point algorithm  
 983 (Algorithm 3) can cover the ideal set, as analyzed in Sec-  
 984 tion V-C1. Similarly, our algorithm with preprocessing can  
 985 obtain the same scheme without processing in each case. The  
 986 Q-learning with preprocessing can find the optimal scheme in  
 987 more scenarios than the one without preprocessing, indicating  
 988 that our preprocessing algorithm can improve the performance  
 989 of Q-learning by reducing the size of the solution space, and thus  
 990 enhance the probability of finding a better state. For PSO-GA  
 991 and GA, the performance is significantly improved in all cases  
 992 with preprocessing, although the optimal solution cannot be  
 993 obtained. For PSO-GA with processing, the response time of its  
 994 offloading scheme is reduced by 0.8%-19.7% compared to that  
 995 without processing. For GA with processing, the response time  
 996 of its offloading scheme is reduced by 0.7%-22.9% compared  
 997 to that without processing. As the algorithm with processing  
 998 only makes decisions on the cut-point functions, it drastically  
 999 reduces the size of the solution space, allowing the algorithms  
 1000 to find better offloading schemes more efficiently.

TABLE VI  
 COMPARISON OF DECISION TIME

(a) LPRA					
Decision time(ms)	Algorithm	Traversal algorithm	Our algorithm	Q-learning	PSO-GA
Preprocessing					
Without preprocessing	313884	8	431	3173	2138

(b) TDA					
Decision time(ms)	Algorithm	Traversal algorithm	Our algorithm	Q-learning	GA
Preprocessing					
Without preprocessing	232985	7	579	2616	1842
With preprocessing	4159	4	76	452	337

1001 3) *The Time Cost of Decision Algorithm: Setting.* The exper-  
 1002 imental setup is the same as Section V-C2, but we record the  
 1003 decision time to explore their cost.

1004 *Result.* As shown in Table VI, compared to other algorithms,  
 1005 the average decision time of our algorithm is the shortest on  
 1006 both LPRA and TDA. On LPRA, the decision time of our  
 1007 unpreprocessed algorithm is 8ms, which saves 98.1%-99.9%  
 1008 compared to other unpreprocessed algorithms. Moreover, the  
 1009 decision time of our preprocessed algorithm is 3ms, which saves  
 1010 93.6%-99.9% compared to other preprocessed algorithms. On  
 1011 TDA, the decision time of our unpreprocessed algorithm is 7ms,  
 1012 which saves 98.8%-99.9% compared to other unpreprocessed  
 1013 algorithms. Moreover, the decision time of our preprocessed  
 1014 algorithm is 4ms, which saves 94.7%-99.9% compared to other  
 1015 preprocessed algorithms.

1016 For both preprocessed and unpreprocessed algorithms, our  
 1017 algorithm, Q-learning, PSO-GA, and GA reduced the costs  
 1018 of the traversal algorithm by 99.5%, 62.5%, 89.1%, 87.8%  
 1019 and 85.7% on LPRA, and 98.2%, 42.6%, 86.9%, 82.7% and  
 1020 81.7% on TDA, respectively. Our preprocessing step extracts  
 1021 cut-point functions, reducing the search space and decision  
 1022 times (Section V-C1 for more details). As a result, our pre-  
 1023 processing effectively improves the performance of all decision  
 1024 algorithms.

## VI. DISCUSSION

### A. Extending to Other Applications

1025 Our work focuses on object-oriented applications in Java. Our  
 1026 algorithm is mainly designed for the call-and-return applica-  
 1027 tions, and it needs to be extended to other styles of applica-  
 1028 tions (e.g., workflow applications and DNN-based applica-  
 1029 tions). For example, in a workflow application, a function *B* is called by  
 1030 function *A*, but passes its execution result to a function *C*. On  
 1031 one hand, the offloading mechanism proposed in this paper  
 1032 can be extended to different types of applications. To support  
 1033 the applications offloading at function granularity in MEC, the  
 1034 statelessness of functions is of utmost importance, since it needs  
 1035 to avoid the loss of state information when the environment  
 1036 changes. For example, each neural network layer of the DNN  
 1037 model can be considered as a stateless function, since all parame-  
 1038 ters required for the computation of each layer are directly passed  
 1039 in through the input. This style is simpler than OO applica-  
 1040 tions

because it does not require any additional transformation. On the other hand, the cut-point function extraction (Algorithm 3) can be extended to other types of applications to reduce the decision overhead. For example, fully connected layers in DNN models, which usually have high execution latency, are suitable to be offloaded and can be considered as cut-points. And neural networks with low execution latency and high data transmission, such as activation layers, are more suitable to be executed on the same computing node as their preceding layers.

### 1051 B. Evaluating in Real-World Environments

1052 In our evaluations, we established an MEC environment  
 1053 to maximize the simulation of the real-world environment.  
 1054 The two mobile devices represent low-performance and high-  
 1055 performance devices, and the network conditions between the  
 1056 mobile devices and the remote servers vary by locations. The  
 1057 results reveal the effectiveness of our approach. The differences  
 1058 between our MEC environment and the real-world environments  
 1059 are that: (1) the application runs in a single-user environment.  
 1060 Therefore, the execution time of each call to the same class of  
 1061 methods on the same computing node is generally close to their  
 1062 average; (2) Our mobility model for mobile devices is simplified.  
 1063 We ignore the wireless fading channel caused by device move-  
 1064 ments, so the network conditions between a mobile device and  
 1065 the same remote server in the same location are generally close  
 1066 to their average. Despite the above differences, our approach  
 1067 can still work in the real-world environment, just with some  
 1068 performance difference. In addition, this study focuses primarily  
 1069 on supporting the dynamic offloading of applications in MEC at  
 1070 function granularity; the two issues above are orthogonal to the  
 1071 problem in this study. In future work, we will consider the above  
 1072 factors, such as supporting multi-user cases via game-theoretic  
 1073 models [39], [40] and supporting complex mobility models  
 1074 through other offloading decision algorithms [32], [41].

## 1075 VII. CONCLUSION

1076 To make use of the scattered and changing computing re-  
 1077 sources in MEC, this paper proposes an adaptive offloading  
 1078 approach, called FUNOff, which supports the offloading at the  
 1079 granularity of functions. For an object-oriented application, it  
 1080 extracts a call tree through code analysis, and takes a preprocess-  
 1081 ing step to find the function invocations suitable for offloading.  
 1082 Next, FUNOff translates such functions to a specific program  
 1083 structure that allows remote access. Finally, it generates an  
 1084 offloading scheme at runtime according to the context of the  
 1085 mobile device, and sends functions to multiple devices according  
 1086 to the offloading scheme. Our evaluations on real applications  
 1087 show that FUNOff significantly improves the performance of  
 1088 applications. In addition, the results show that the offloading  
 1089 at the granularity of functions is more suitable for computation  
 1090 offloading in MEC, and our preprocessing effectively improves  
 1091 the performance of offloading decision algorithms.

## REFERENCES

- [1] Z. Su, Y. Hui, and T. H. Luan, "Distributed task allocation to enable collaborative autonomous driving with network softwarization," *IEEE J. Sel. Areas Commun.*, vol. 36, no. 10, pp. 2175–2189, Oct. 2018.
- [2] C. Liu et al., "A new deep learning-based food recognition system for dietary assessment on an edge computing service infrastructure," *IEEE Trans. Services Comput.*, vol. 11, no. 2, pp. 249–261, Mar./Apr. 2018.
- [3] T. Braud, F. H. Bijarbooneh, D. Chatzopoulos, and P. Hui, "Future networking challenges: The case of mobile augmented reality," in *Proc. IEEE 37th Int. Conf. Distrib. Comput. Syst.*, 2017, pp. 1796–1807.
- [4] T. Zhao, J. Liu, Y. Wang, H. Liu, and Y. Chen, "Towards low-cost sign language gesture recognition leveraging wearables," *IEEE Trans. Mobile Comput.*, vol. 20, no. 4, pp. 1685–1701, Apr. 2021.
- [5] F. Yang, J. Li, T. Lei, and S. Wang, "Architecture and key technologies for Internet of Vehicles: A survey," *IEEE J. Commun. Inf. Netw.*, vol. 2, no. 2, pp. 1–17, 2017.
- [6] S. Jeong, O. Simeone, and J. Kang, "Mobile edge computing via a UAV-mounted cloudlet: Optimization of bit allocation and path planning," *IEEE Trans. Veh. Technol.*, vol. 67, no. 3, pp. 2049–2063, Mar. 2018.
- [7] I. A. Elgendi, W. Zhang, Y.-C. Tian, and K. Li, "Resource allocation and computation offloading with data security for mobile edge computing," *Future Gener. Comput. Syst.*, vol. 100, pp. 531–541, 2019.
- [8] P. Mach and Z. Becvar, "Mobile edge computing: A survey on architecture and computation offloading," *IEEE Commun. Surveys Tut.*, vol. 19, no. 3, pp. 1628–1656, Third Quarter 2017.
- [9] E. Cuervo et al., "MAUI: Making smartphones last longer with code offload," in *Proc. Int. Conf. Mobile Syst., Appl. Serv.*, 2010, pp. 49–62.
- [10] B.-G. Chun, S. Ihm, P. Maniatis, M. Naik, and A. Patti, "CloneCloud: Elastic execution between mobile device and cloud," in *Proc. Conf. Comput. Syst.*, 2011, pp. 301–314.
- [11] R. Kemp, N. Palmer, T. Kielmann, and H. Bal, "Cuckoo: A computation offloading framework for smartphones," in *Proc. Int. Conf. Mobile Syst., Appl. Serv.*, 2012, pp. 59–79.
- [12] J. Pan and J. McElhannon, "Future edge cloud and edge computing for Internet of Things applications," *IEEE Internet of Things J.*, vol. 5, no. 1, pp. 439–449, Feb. 2018.
- [13] H. Guo, J. Liu, and J. Lv, "Toward intelligent task offloading at the edge," *IEEE Netw.*, vol. 34, no. 2, pp. 128–134, Mar./Apr. 2020.
- [14] T. X. Tran, A. Hajisami, P. Pandey, and D. Pompili, "Collaborative mobile edge computing in 5G networks: New paradigms, scenarios, and challenges," *IEEE Commun. Mag.*, vol. 55, no. 4, pp. 54–61, Apr. 2017.
- [15] W. Shi, J. Cao, Q. Zhang, Y. Li, and L. Xu, "Edge computing: Vision and challenges," *IEEE Internet Things J.*, vol. 3, no. 5, pp. 637–646, Oct. 2016.
- [16] W. Chen, D. Wang, and K. Li, "Multi-user multi-task computation offloading in green mobile edge cloud computing," *IEEE Trans. Services Comput.*, vol. 12, no. 5, pp. 726–738, Sep./Oct. 2019.
- [17] Y. Mao, C. You, J. Zhang, K. Huang, and K. B. Letaief, "A survey on mobile edge computing: The communication perspective," *IEEE Commun. Surveys Tut.*, vol. 19, no. 4, pp. 2322–2358, Fourth Quarter 2017.
- [18] P. Zhao, H. Tian, K.-C. Chen, S. Fan, and G. Nie, "Context-aware TDD configuration and resource allocation for mobile edge computing," *IEEE Trans. Commun.*, vol. 68, no. 2, pp. 1118–1131, Feb. 2020.
- [19] X. Hou et al., "Reliable computation offloading for edge-computing-enabled software-defined IoV," *IEEE Internet Things J.*, vol. 7, no. 8, pp. 7097–7111, Aug. 2020.
- [20] J. L. D. Neto, S.-Y. Yu, D. F. Macedo, J. M. S. Nogueira, R. Langar, and S. Secci, "ULOOF: A user level online offloading framework for mobile edge computing," *IEEE Trans. Mobile Comput.*, vol. 17, no. 11, pp. 2660–2674, Nov. 2018.
- [21] M. Golkarifard, J. Yang, Z. Huang, A. Movaghar, and P. Hui, "Dandelion: A unified code offloading system for wearable computing," *IEEE Trans. Mobile Comput.*, vol. 18, no. 3, pp. 546–559, Mar. 2019.
- [22] M. Xu, F. Qian, M. Zhu, F. Huang, S. Pushp, and X. Liu, "DeepWear: Adaptive local offloading for on-wearable deep learning," *IEEE Trans. Mobile Comput.*, vol. 19, no. 2, pp. 314–330, Feb. 2020.
- [23] X. Chen, J. Chen, B. Liu, Y. Ma, and H. Zhong, "AndroidOff: Offloading Android application based on cost estimation," *J. Syst. Softw.*, vol. 158, 2019, Art. no. 110418.
- [24] X. Chen, S. Chen, M. A. Yun, B. Liu, Y. Zhang, and G. Huang, "An adaptive offloading framework for Android applications in mobile edge computing," *SCIENCE CHINA Inf. Sci.*, vol. 062, no. 008, pp. 110–126, 2019.

- 1167 [25] L. Bao, C. Wu, X. Bu, N. Ren, and M. Shen, "Performance modeling and  
1168 workflow scheduling of microservice-based applications in clouds," *IEEE Trans. Parallel Distrib. Syst.*, vol. 30, no. 9, pp. 2114–2129, Sep. 2019.  
1169
- 1170 [26] G. A. S. Cassel et al., "Serverless computing for Internet of Things: A systematic literature review," *Future Gener. Comput. Syst.*, vol. 128, pp. 299–316, 2022.  
1171
- 1172 [27] P. Castro, V. Ishakian, V. Muthusamy, and A. Slominski, "The rise of serverless computing," *Commun. ACM*, vol. 62, no. 12, pp. 44–54, 2019.  
1173
- 1174 [28] S. Hendrickson, S. Sturdevant, T. Harter, V. Venkataramani, A. C. Arpacı-Dusseau, and R. H. Arpacı-Dusseau, "Serverless computation with Open-Lambda," in *Proc. 8th USENIX Workshop Hot Topics Cloud Comput.*, 2016, pp. 33–39.  
1175
- 1176 [29] Y. Zhang, G. Huang, X. Liu, W. Zhang, H. Mei, and S. Yang, "Refactoring Android Java code for on-demand computation offloading," *ACM SIGPLAN Notices*, vol. 47, no. 10, pp. 233–248, 2012.  
1177
- 1178 [30] Z. Cheng, P. Li, J. Wang, and S. Guo, "Just-in-time code offloading for wearable computing," *IEEE Trans. Emerg. Topics Comput.*, vol. 3, no. 1, pp. 74–83, Mar. 2015.  
1179
- 1180 [31] X. Chen, J. Zhang, B. Lin, Z. Chen, K. Wolter, and G. Min, "Energy-efficient offloading for DNN-based smart IoT systems in cloud-edge environments," *IEEE Trans. Parallel Distrib. Syst.*, vol. 33, no. 3, pp. 683–697, Mar. 2022.  
1181
- 1182 [32] Y. Du, J. Li, L. Shi, T. Liu, F. Shu, and Z. Han, "Two-tier matching game in small cell networks for mobile edge computing," *IEEE Trans. Services Comput.*, vol. 15, no. 1, pp. 254–265, Jan./Feb. 2022.  
1183
- 1184 [33] M. Altamimi, A. Abdrabou, K. Naik, and A. Nayak, "Energy cost models of smartphones for task offloading to the cloud," *IEEE Trans. Emerg. Topics Comput.*, vol. 3, no. 3, pp. 384–398, Sep. 2015.  
1185
- 1186 [34] K. Elgazzar, P. Martin, and H. S. Hassanein, "Cloud-assisted computation offloading to support mobile services," *IEEE Trans. Cloud Comput.*, vol. 4, no. 3, pp. 279–292, Third Quarter 2016.  
1187
- 1188 [35] B. Zhou, A. V. Dashtjerdi, R. N. Calheiros, S. N. Srivama, and R. Buyya, "mCloud: A context-aware offloading framework for heterogeneous mobile cloud," *IEEE Trans. Services Comput.*, vol. 10, no. 5, pp. 797–810, Sep./Oct. 2017.  
1189
- 1190 [36] H. Wu, W. J. Knottenbelt, and K. Wolter, "An efficient application partitioning algorithm in mobile environments," *IEEE Trans. Parallel Distrib. Syst.*, vol. 30, no. 7, pp. 1464–1480, Jul. 2019.  
1191
- 1192 [37] P. Civicioglu, "Backtracking search optimization algorithm for numerical optimization problems," *Appl. Math. Comput.*, vol. 219, no. 15, pp. 8121–8144, 2013.  
1193
- 1194 [38] R. S. Sutton and A. G. Barto, *Reinforcement Learning: An Introduction*. Cambridge, MA, USA: MIT Press, 2018.  
1195
- 1196 [39] P. A. Apostolopoulos, E. E. Tsirropoulou, and S. Papavassiliou, "Risk-aware data offloading in multi-server multi-access edge computing environment," *IEEE/ACM Trans. Netw.*, vol. 28, no. 3, pp. 1405–1418, Jun. 2020.  
1197
- 1198 [40] P. K. Bishoyi and S. Misra, "Enabling green mobile-edge computing for 5G-based healthcare applications," *IEEE Trans. Green Commun. Netw.*, vol. 5, no. 3, pp. 1623–1631, Sep. 2021.  
1199
- 1200 [41] Y. Li, D. Guo, Y. Zhao, X. Cao, and H. Chen, "Efficient risk-averse request allocation for multi-access edge computing," *IEEE Commun. Lett.*, vol. 25, no. 2, pp. 533–537, Feb. 2021.  
1201



**Xing Chen** (Member, IEEE) received the BS and PhD degrees from Peking University, in 2008 and 2013, respectively. He is a professor with Fuzhou University, and the director of Fujian Key Laboratory of Network Computing and Intelligent Information Processing. He joined Fuzhou University since 2013. He focuses on the software systems and engineering approaches for cloud and mobility. His current projects cover the topics from self-adaptive software, computation offloading, model driven approach and so on. He has published more than 80 journal and conference articles, including *IEEE Transactions on Parallel and Distributed Systems*, *IEEE Transactions on Cloud Computing*, *IEEE Transactions on Industrial Informatics*, etc. He obtained the Natural Science Fund of Fujian for Distinguished Young Scholars and the Program of Fujian for the Top Young Talents. He was awarded two First Class Prizes for Provincial Scientific and Technological Progress, separately, in 2018 and 2020.

1220  
1221  
1222  
1223  
1224  
1225  
1226  
1227  
1228  
1229  
1230  
1231  
1232  
1233  
1234  
1235  
1236  
1237



**Ming Li** received the BS degree in computer science and technology from Fuzhou University, Fujian, China, in 2019, where he is currently working toward the PhD degree in computer technology with the College of Mathematics and Computer Science, Fuzhou University. He has also been a part of the Fujian Key Laboratory of Network Computing and Intelligent Information Processing, Fuzhou University, since September 2019. His current research interests include system software, and edge computing.

1238  
1239  
1240  
1241  
1242  
1243  
1244  
1245  
1246  
1247  
1248



**Hao Zhong** (Member, IEEE) received the MS and PhD degrees from Peking University in 2005 and 2009, respectively. He is an associate professor with Shanghai Jiao Tong University. His research interest is the area of software engineering. He served on the program committees of reputable venues such as ICSE, ESEC/FSE, ASE, OOPSLA, ICSME, MSR and COMPSAC. He is a recipient of ACM SIGSOFT Distinguished Paper Award, the best paper award of ASE, and the best paper award of APSEC.

1249  
1250  
1251  
1252  
1253  
1254  
1255  
1256  
1257  
1258  
1259



**Xiaona Chen** received the BS degree in software engineering from Fuzhou University, Fujian, China, in 2019. She is currently working toward the MS degree in software engineering with the College of Mathematics and Computer Science, Fuzhou University. She has also been a part of the Fujian Key Laboratory of Network Computing and Intelligent Information Processing, Fuzhou University, since September 2019. Her current research interests include system software, and computation offloading.

1260  
1261  
1262  
1263  
1264  
1265  
1266  
1267  
1268  
1269  
1270



**Yun Ma** (Member, IEEE) received the PhD degree majoring in computer science from the School of EECS, Peking University, under the direction of professor Hong Mei and professor Gang Huang. His research interests lie in mobile computing, Web technologies, and services computing. Currently, he focuses on synergy between the mobile and the Web, trying to improve the mobile user experience by leveraging the best practices from native apps and Web apps.

1271  
1272  
1273  
1274  
1275  
1276  
1277  
1278  
1279  
1280  
1281



**Ching-Hsien Hsu** (Senior Member, IEEE) is a chair professor and the dean of the College of Information and Electrical Engineering, Asia University, Taiwan. His research includes high-performance computing, cloud computing, parallel and distributed systems, Big Data analytics, ubiquitous/pervasive computing, and intelligence. He has published 100 papers in top journals such as *IEEE Transactions on Parallel and Distributed Systems*, *IEEE Transactions on Services Computing*, *IEEE Transactions on Cloud Computing*, *IEEE Transactions on Emerging Topics in Computing*, *IEEE System*, *IEEE Network*, *ACM Transactions on Multimedia Computing, Communications, and Applications* and book chapters in these areas.

1282  
1283  
1284  
1285  
1286  
1287  
1288  
1289  
1290  
1291  
1292  
1293  
1294  
1295